

Dynamics of Berry-phase polarization in time-dependent electric fields

Ivo Souza, Jorge Íñiguez,* and David Vanderbilt

Department of Physics and Astronomy, Rutgers University, Piscataway, New Jersey 08854-8019, USA

(Received 1 August 2003; published 20 February 2004)

We consider the flow of polarization current $\mathbf{J} = d\mathbf{P}/dt$ produced by a homogeneous electric field $\mathcal{E}(t)$ or by rapidly varying some other parameter in the Hamiltonian of a solid. For an initially insulating system and a collisionless time evolution, the dynamic polarization $\mathbf{P}(t)$ is given by a nonadiabatic version of the King-Smith–Vanderbilt geometric-phase formula. This leads to a computationally convenient form for the Schrödinger equation where the electric field is described by a linear scalar potential handled on a discrete mesh in reciprocal space. Stationary solutions in sufficiently weak static fields are local minima of the energy functional of Nunes and Gonze. Such solutions only exist below a critical field that depends inversely on the density of k points. For higher fields they become long-lived resonances, which can be accessed dynamically by gradually increasing \mathcal{E} . As an illustration the dielectric function in the presence of a dc bias field is computed for a tight-binding model from the polarization response to a step-function discontinuity in $\mathcal{E}(t)$, displaying the Franz-Keldysh effect.

DOI: 10.1103/PhysRevB.69.085106

PACS number(s): 71.15.Qe, 78.20.Bh

I. INTRODUCTION

A very successful theoretical and computational framework was developed by King-Smith and Vanderbilt¹ for dealing within periodic boundary conditions with the macroscopic dielectric polarization of an insulator. The central result of the theory of bulk polarization (TBP) is an expression for the electronic contribution \mathbf{P} which takes the form of a Berry's phase² of the valence-band Bloch wave functions transported across the Brillouin zone (BZ). Alternatively, it can be recast in real space as the vector sum of the centers of charge of the valence-band Wannier functions. Practical prescriptions were devised for computing both the Berry's phase¹ and the Wannier functions,³ which have become standard features of first-principles electronic structure codes.

The measurable quantity accessed by the TBP is the change $\Delta\mathbf{P}$ in macroscopic polarization induced by changing some parameter λ in the electronic Hamiltonian $\hat{H}(t) = \hat{H}[\lambda(t)]$. The following assumptions were explicitly made in the original derivation.¹ (i) Adiabaticity: the change in $\lambda(t)$ is slow enough such that the electrons remain in the instantaneous ground state of $\hat{H}(t)$, apart from small deviations proportional to $d\lambda/dt$ described by first-order adiabatic perturbation theory; (ii) the ground state of $\hat{H}(t)$ remains insulating at all times, separated from excited states by finite energy gaps; and (iii) $\hat{H}(t)$ is lattice periodic. The first two assumptions are related in that the size of the energy gap sets the scale for deviations from adiabaticity.

A spatially homogeneous electric field necessarily violates either (i) or (iii): if the field is introduced via a vector potential $\mathbf{A}(t) = -c \int^t \mathcal{E}(t') dt'$, $\hat{H}(t)$ remains lattice periodic but changes nonadiabatically, even for a static field; if instead a scalar-potential term $e\mathcal{E}(t) \cdot \hat{\mathbf{r}}$ is used, $\hat{H}(t)$ is no longer lattice periodic. Nevertheless, the TBP has been successfully applied to situations where electric fields are present,^{4–10} but a rigorous justification for doing so is still lacking.

In this paper we reexamine the TBP and find that it can be

generalized as follows. Assumption (i) can be dropped altogether. Assumption (ii) is only invoked at $t=0$; the ensuing nonadiabatic dynamics may admix considerable amounts of excited states into the occupied subspace. Finally assumption (iii) can be relaxed to allow for a linear scalar potential to be present in addition to the periodic crystal potential.

These generalizations extend the scope of the TBP to *nonadiabatic* polarization currents induced by time-dependent electric fields, or by other rapid changes in $\hat{H}(t)$ (e.g., the initial nonthermal ionic motion that accompanies photoexcitation of the electrons by an intense laser pulse¹¹). The dynamical equations for the electrons that come out of this generalized TBP are derived and applied in the context of a tight-binding model. These equations are semiclassical (the electrons are treated quantum mechanically, whereas the electric field is treated classically) and nonperturbative (electric fields of finite magnitude are allowed).

We begin by considering in Sec. II some general properties of the coherent dynamics of Bloch electrons that are initially in an insulating state. They are used in Sec. III to discuss the macroscopic current $\mathbf{J}(t)$, which is expressed as the rate of change of a dynamic polarization $\mathbf{P}(t)$ given by nonadiabatic versions of the King-Smith–Vanderbilt expressions. In Sec. IV we derive from this generalized TBP a numerically convenient form for the time-dependent Schrödinger equation (TDSE) in the scalar-potential gauge, discretized on a mesh of k points. Stable stationary solutions in static fields are discussed in Sec. V. They exist only below a critical field \mathcal{E}_c which decreases with increasing k -point density, and are local minima of the energy functional of Nunes and Gonze.^{7–9} A prescription is given for computing them using an iterative diagonalization scheme. In Sec. VI we show numerically on a tight-binding model how the regime above the critical field can be accessed dynamically, by gradually increasing the electric field beyond the critical value. We also compute the dielectric function of the same model in the presence of a static bias field, displaying the Franz-Keldysh effect.

II. GENERAL PROPERTIES OF THE DYNAMICS

A. Lattice periodicity

Here we expound in more detail an argument, sketched in Ref. 8, that makes use of the one-particle density matrix to handle the presence of electric fields in a well-controlled fashion.¹² We say that the one-particle density matrix $n(\mathbf{r}, \mathbf{r}') = \langle \mathbf{r} | \hat{n} | \mathbf{r}' \rangle$ is lattice periodic if

$$n(\mathbf{r}, \mathbf{r}') = n(\mathbf{r} + \mathbf{R}, \mathbf{r}' + \mathbf{R}), \quad (1)$$

where \mathbf{R} is a lattice vector. In particular, this implies periodicity of the charge density. Suppose that Eq. (1) is true at $t = 0$ [e.g., the electrons are in the ground state of the crystal Hamiltonian $\hat{H}^0(t=0)$]. At that time a homogeneous electric field is turned on, which may subsequently have an arbitrarily strong and rapid variation; $\hat{H}^0(t)$ may also undergo arbitrarily rapid variations (but must remain periodic). The full Hamiltonian in the scalar-potential gauge is

$$\hat{H}(t) = \hat{H}^0(t) + \hat{H}^{\mathcal{E}}(t), \quad (2)$$

where $\hat{H}^{\mathcal{E}}(t) = e\mathcal{E}(t) \cdot \hat{\mathbf{r}}$ describes the electric field in the dipole approximation and $-e$ is the electron charge.

Let us show that in the absence of scattering the lattice periodicity of $n(\mathbf{r}, \mathbf{r}')$ is preserved at all later times. It suffices to establish that $\dot{n}(\mathbf{r}, \mathbf{r}') = \dot{n}(\mathbf{r} + \mathbf{R}, \mathbf{r}' + \mathbf{R})$. The density matrix evolves according to $i\hbar d\hat{n}/dt = [\hat{H}, \hat{n}]$, or, in the position representation,

$$i\hbar \dot{n}(\mathbf{r}, \mathbf{r}') = \int [H(\mathbf{r}, \mathbf{x})n(\mathbf{x}, \mathbf{r}') - n(\mathbf{r}, \mathbf{x})H(\mathbf{x}, \mathbf{r}')] d\mathbf{x}. \quad (3)$$

(When left unspecified, the domain of integration over spatial coordinates is understood to be the entire space.) For clarity we consider the effect of \hat{H}^0 and $\hat{H}^{\mathcal{E}}$ separately. The \hat{H}^0 term yields

$$i\hbar \dot{n}(\mathbf{r} + \mathbf{R}, \mathbf{r}' + \mathbf{R}) = \int [H^0(\mathbf{r} + \mathbf{R}, \mathbf{x})n(\mathbf{x}, \mathbf{r}' + \mathbf{R}) - n(\mathbf{r} + \mathbf{R}, \mathbf{x})H^0(\mathbf{x}, \mathbf{r}' + \mathbf{R})] d\mathbf{x}. \quad (4)$$

Making the change of variables $\mathbf{x}' = \mathbf{x} - \mathbf{R}$ and invoking the lattice periodicity of \hat{H}^0 and \hat{n} , we find $\dot{n}(\mathbf{r} + \mathbf{R}, \mathbf{r}' + \mathbf{R}) = \dot{n}(\mathbf{r}, \mathbf{r}')$. Using $\mathbf{r}(\mathbf{r}, \mathbf{r}') = \langle \mathbf{r} | \hat{\mathbf{r}} | \mathbf{r}' \rangle = \mathbf{r} \delta(\mathbf{r} - \mathbf{r}')$ the contribution from $\hat{H}^{\mathcal{E}}$ is seen to have the same property:

$$\begin{aligned} i\hbar \dot{n}(\mathbf{r} + \mathbf{R}, \mathbf{r}' + \mathbf{R}) &= e\mathcal{E} \cdot (\mathbf{r} + \mathbf{R}) n(\mathbf{r} + \mathbf{R}, \mathbf{r}' + \mathbf{R}) \\ &\quad - e\mathcal{E} \cdot (\mathbf{r}' + \mathbf{R}) n(\mathbf{r} + \mathbf{R}, \mathbf{r}' + \mathbf{R}) \\ &= e\mathcal{E} \cdot (\mathbf{r} - \mathbf{r}') n(\mathbf{r}, \mathbf{r}') = i\hbar \dot{n}(\mathbf{r}, \mathbf{r}'). \end{aligned} \quad (5)$$

Hence $n(\mathbf{r}, \mathbf{r}')$ remains lattice periodic under the action of the full Hamiltonian (2). This was to be expected, since in the vector-potential gauge the Hamiltonian is periodic.¹³ The purpose of this exercise was to show explicitly how this re-

sult comes about in the scalar-potential gauge, where the nonperiodicity of \hat{H} has been a source of some confusion regarding this issue.

B. Wannier representability

The previous result on the conservation of lattice periodicity is valid for both metals and insulators. In what follows we shall specialize to the case where the system is initially in an insulating state, in which case a stronger statement can be made regarding the nature of the states at $t > 0$.

We will assume the absence of spin degeneracy throughout, so that states are singly occupied. In terms of the valence Bloch eigenstates of $\hat{H}^0(t=0)$, the initial density matrix is

$$n(\mathbf{r}, \mathbf{r}'; t=0) = \Omega_B^{-1} \sum_{n=1}^M \int d\mathbf{k} \psi_{\mathbf{k}n}(\mathbf{r}) \psi_{\mathbf{k}n}^*(\mathbf{r}'), \quad (6)$$

where the integral is over the BZ of volume $\Omega_B = (2\pi)^3/v$, and M is the number of filled bands. [Clearly, such a density matrix is lattice periodic. Its idempotency can be checked using Eq. (A1).] We shall prove that, as the density matrix evolves in time according to

$$i\hbar \dot{n}(\mathbf{r}, \mathbf{r}'; t) = \langle \mathbf{r} | [\hat{H}^0 + \hat{H}^{\mathcal{E}}, \hat{n}] | \mathbf{r}' \rangle, \quad (7)$$

it can still be expressed in the same form,

$$n(\mathbf{r}, \mathbf{r}'; t) = \Omega_B^{-1} \sum_{n=1}^M \int d\mathbf{k} \phi_{\mathbf{k}n}(\mathbf{r}, t) \phi_{\mathbf{k}n}^*(\mathbf{r}', t). \quad (8)$$

Although at $t > 0$ the occupied states $\phi_{\mathbf{k}n}(\mathbf{r}, t)$ may depart significantly from the valence states of $\hat{H}^0(t)$, they remain orthonormal and *Bloch-like*: $\phi_{\mathbf{k}n}(\mathbf{r}, t) = e^{i\mathbf{k} \cdot \mathbf{r}} v_{\mathbf{k}n}(\mathbf{r}, t)$, with $v_{\mathbf{k}n}(\mathbf{r} + \mathbf{R}, t) = v_{\mathbf{k}n}(\mathbf{r}, t)$.

The cell-periodic states $v_{\mathbf{k}n}(\mathbf{r}, t)$ are the central objects in our formalism. For discussion purposes only, let us expand them in the set of eigenstates $u_{\mathbf{k}m}(\mathbf{r}, t) = e^{-i\mathbf{k} \cdot \mathbf{r}} \psi_{\mathbf{k}m}(\mathbf{r}, t)$ of the cell-periodic Hamiltonian $\hat{H}_{\mathbf{k}}^0(t) = e^{-i\mathbf{k} \cdot \hat{\mathbf{r}}} \hat{H}^0(t) e^{i\mathbf{k} \cdot \hat{\mathbf{r}}}$:

$$|v_{\mathbf{k}n}(t)\rangle = \sum_{m=1}^{\infty} c_{\mathbf{k}, nm}(t) |u_{\mathbf{k}m}(t)\rangle. \quad (9)$$

Individual eigenstates will in general have fractional occupations $0 \leq n_{\mathbf{k}m} = \sum_{n=1}^M |c_{\mathbf{k}, nm}|^2 \leq 1$ at $t > 0$, but the total population $n_{\mathbf{k}} = \sum_{m=1}^{\infty} n_{\mathbf{k}m}$ is the same for every \mathbf{k} and equals the number of filled bands at $t=0$. This is intuitively clear, since a spatially homogeneous electric field causes vertical transitions in k space which amount to a redistribution of the electron population among states with equal \mathbf{k} ; the same is true for the transitions induced by varying the lattice periodic $\hat{H}^0(t)$.

We will justify Eq. (8) by deriving a dynamics for the $|v_{\mathbf{k}n}\rangle$ that ensures that Eq. (8) provides a solution to Eq. (7). Since there is a gauge freedom

$$|v_{\mathbf{k}n}\rangle \rightarrow \sum_{m=1}^M U_{\mathbf{k}, mn} |v_{\mathbf{k}m}\rangle \quad (10)$$

($U_{\mathbf{k}}$ is a \mathbf{k} -dependent unitary $M \times M$ matrix) in the definition of the $|v_{\mathbf{k}n}\rangle$,³ the evolution equation for them is not unique. We require only that the $|v_{\mathbf{k}n}\rangle$ should yield the correct dynamics for the gauge-invariant density matrix, Eq. (7), and we will look for the simplest solution that achieves this goal.

By hypothesis, at time t $\dot{n}(\mathbf{r}, \mathbf{r}')$ takes the form

$$\begin{aligned} \dot{n}(\mathbf{r}, \mathbf{r}') = & \Omega_B^{-1} \sum_{n=1}^M \int d\mathbf{k} e^{i\mathbf{k} \cdot (\mathbf{r} - \mathbf{r}')} [\dot{v}_{\mathbf{k}n}(\mathbf{r}) v_{\mathbf{k}n}^*(\mathbf{r}') \\ & + v_{\mathbf{k}n}(\mathbf{r}) \dot{v}_{\mathbf{k}n}^*(\mathbf{r}')]. \end{aligned} \quad (11)$$

As in the preceding section, we consider the contributions from \hat{H}^0 and $\hat{H}^{\mathcal{E}}$ in Eq. (7) separately. The former is captured by $i\hbar|\dot{v}_{\mathbf{k}n}\rangle = \hat{H}_{\mathbf{k}}^0|v_{\mathbf{k}n}\rangle$. To deal with $\hat{H}^{\mathcal{E}}$ we resort to manipulations familiar from the crystal-momentum representation¹⁴ (CMR) (but with the crucial difference that in the CMR those manipulations are applied to the $|u_{\mathbf{k}n}\rangle$, not to the $|v_{\mathbf{k}n}\rangle$). We first observe that

$$\begin{aligned} \langle \mathbf{r} | [\hat{\mathbf{r}}, \hat{n}] | \mathbf{r}' \rangle &= (\mathbf{r} - \mathbf{r}') n(\mathbf{r}, \mathbf{r}') \\ &= \Omega_B^{-1} \sum_{n=1}^M \int d\mathbf{k} v_{\mathbf{k}n}(\mathbf{r}) v_{\mathbf{k}n}^*(\mathbf{r}') \\ &\quad \times (-i \partial_{\mathbf{k}}) e^{i\mathbf{k} \cdot (\mathbf{r} - \mathbf{r}')}. \end{aligned} \quad (12)$$

Integrating by parts and noting that in a *periodic gauge* ($\phi_{\mathbf{k}+\mathbf{G},n} = \phi_{\mathbf{k}n}$) the boundary term vanishes, we obtain

$$\begin{aligned} \langle \mathbf{r} | [\hat{H}^{\mathcal{E}}, \hat{n}] | \mathbf{r}' \rangle &= \Omega_B^{-1} \sum_{n=1}^M \int d\mathbf{k} e^{i\mathbf{k} \cdot (\mathbf{r} - \mathbf{r}')} i e \mathcal{E} \cdot \{ [\partial_{\mathbf{k}} v_{\mathbf{k}n}(\mathbf{r})] v_{\mathbf{k}n}^*(\mathbf{r}') \\ &\quad + v_{\mathbf{k}n}(\mathbf{r}) [\partial_{\mathbf{k}} v_{\mathbf{k}n}^*(\mathbf{r}')] \}. \end{aligned} \quad (13)$$

Comparing with Eqs. (7) and (11) we arrive at $i\hbar|\dot{v}_{\mathbf{k}n}\rangle = i e \mathcal{E} \cdot \partial_{\mathbf{k}} |v_{\mathbf{k}n}\rangle$. The effect of $\hat{H}^{\mathcal{E}}$ thus takes the form of a k derivative, and the combined effect of \hat{H}^0 and $\hat{H}^{\mathcal{E}}$ is

$$i\hbar|\dot{v}_{\mathbf{k}n}\rangle = (\hat{H}_{\mathbf{k}}^0 + i e \mathcal{E} \cdot \partial_{\mathbf{k}}) |v_{\mathbf{k}n}\rangle. \quad (14)$$

This is our version of the TDSE for Bloch electrons in the scalar-potential gauge, constructed in order that Eq. (8) will satisfy Eq. (7). The time-independent version was introduced as an *ansatz* in Ref. 7.¹⁵ The equivalence of Eq. (14) to other forms in the literature is established in Appendix A.

If at time t the M states $|v_{\mathbf{k}n}\rangle$ at every \mathbf{k} are lattice periodic and orthonormal, the dynamics dictated by Eq. (14) preserves those properties, i.e., $\dot{v}_{\mathbf{k}n}(\mathbf{r} + \mathbf{R}) = \dot{v}_{\mathbf{k}n}(\mathbf{r})$ and $d\langle v_{\mathbf{k}n} | v_{\mathbf{k}n} \rangle / dt = 0$. This can be seen as follows. Starting from

$$\begin{aligned} i\hbar \dot{v}_{\mathbf{k}n}(\mathbf{r} + \mathbf{R}) &= \int H_{\mathbf{k}}^0(\mathbf{r} + \mathbf{R}, \mathbf{x}) v_{\mathbf{k}n}(\mathbf{x}) d\mathbf{x} \\ &\quad + i e \mathcal{E} \cdot \partial_{\mathbf{k}} v_{\mathbf{k}n}(\mathbf{r} + \mathbf{R}), \end{aligned} \quad (15)$$

making the change of variables $\mathbf{x}' = \mathbf{x} - \mathbf{R}$, and invoking the assumed lattice periodicity of both \hat{H}^0 and $v_{\mathbf{k}n}(\mathbf{r})$, the right-hand side becomes $i\hbar \dot{v}_{\mathbf{k}n}(\mathbf{r})$. As for orthonormality, Eq. (14) yields¹⁶

$$\frac{d}{dt} \langle v_{\mathbf{k}n} | v_{\mathbf{k}n} \rangle = \frac{e}{\hbar} \mathcal{E} \cdot \partial_{\mathbf{k}} \langle v_{\mathbf{k}n} | v_{\mathbf{k}n} \rangle. \quad (16)$$

Since by hypothesis

$$\langle v_{\mathbf{k}n} | v_{\mathbf{k}m} \rangle \equiv \int v_{\mathbf{k}n}^*(\mathbf{r}) v_{\mathbf{k}m}(\mathbf{r}) d\mathbf{r} = \delta_{n,m}, \quad (17)$$

where the integral is over a unit cell, the right-hand side of Eq. (16) vanishes. This completes the proof of Eq. (8).

Two assumptions were made in the above derivation. The first is that the states $|v_{\mathbf{k}n}\rangle$ vary smoothly with \mathbf{k} , so that k derivatives exist; we will come back to this point in Sec. III B. The second is that the dynamics is scattering-free. Note that Eq. (16) is closely related to the collisionless Boltzmann equation; incoherent scattering would destroy the constancy of the total population $n_{\mathbf{k}}$ by inducing transitions between different k points.

Having established that the occupied manifold is spanned by M Bloch-like states at each \mathbf{k} , we now transform them into Wannier-like states $\langle \mathbf{r} | W_{\mathbf{R}n}(t) \rangle = W_n(\mathbf{r} - \mathbf{R}, t)$ in the usual way:

$$|W_{\mathbf{R}n}(t)\rangle = \Omega_B^{-1} \sum_{m=1}^M \int d\mathbf{k} e^{-i\mathbf{k} \cdot \mathbf{R}} U_{\mathbf{k},mn}(t) | \phi_{\mathbf{k}m}(t) \rangle, \quad (18)$$

where a periodic gauge is assumed and we have inserted a unitary rotation (10) among the occupied states. The assumption that by a judicious choice of the matrices $U_{\mathbf{k}}(t)$ the Bloch-like states can be made to vary smoothly with \mathbf{k} is equivalent to the assumption that the Wannier-like states can be chosen to be well localized.³

The density matrix (8) can now be recast as

$$n(\mathbf{r}, \mathbf{r}'; t) = \sum_{n=1}^M \sum_{\mathbf{R}} W_{\mathbf{R}n}(\mathbf{r}, t) W_{\mathbf{R}n}^*(\mathbf{r}', t). \quad (19)$$

We will term *Wannier representable* (WR) a state whose density matrix is of this form. An insulating ground state is WR, while a metallic state is not. We have established that under the Hamiltonian (2) and in the absence of scattering, an initially insulating system remains WR, or “insulating-like,” even if at some later time the ground state of $\hat{H}^0(t)$ becomes metallic.¹⁷ Unlike a true insulating ground state, or a stationary field-polarized state,⁸ a dynamic WR state will in general break time-reversal symmetry and carry a macroscopic current. This is the subject of the following section.

III. DYNAMIC POLARIZATION AND CURRENT

A. Derivation

Our aim in this section is to show that a WR state carries a current that can be expressed as the rate of change of a polarization per unit volume,

$$\mathbf{J}(t) = \frac{d\mathbf{P}(t)}{dt}, \quad (20)$$

where $\mathbf{P}(t)$ is given in a periodic gauge by

$$P_\alpha(t) = -\frac{ie}{(2\pi)^3} \sum_{n=1}^M \int d\mathbf{k} \langle v_{\mathbf{k}n}(t) | \partial_{k_\alpha} v_{\mathbf{k}n}(t) \rangle \quad (21)$$

(α is a Cartesian direction) or, equivalently, by

$$\mathbf{P}(t) = -\frac{e}{v} \sum_{n=1}^M \int \mathbf{r} |W_n(\mathbf{r}, t)|^2 d\mathbf{r}. \quad (22)$$

Equations (21) and (22) are identical to the King-Smith–Vanderbilt expressions appropriate for the adiabatic regime and $\mathcal{E}=0$,¹ except that in Eq. (21) the valence-band eigenstates $|u_{\mathbf{k}n}\rangle$ have been replaced by the instantaneous solutions of the TDSE (14), and the $W_n(\mathbf{r}, t)$ in Eq. (22) are the Wannier states corresponding to $v_{\mathbf{k}n}(\mathbf{r}, t)$. Equation (21) can be interpreted as a nonadiabatic geometric phase.¹⁸

As in the adiabatic case, $\mathbf{P}(t)$ is invariant under the transformation (10) only up to a “quantum of polarization” $(e/v)\mathbf{R}$. Naturally, this gauge indeterminacy does not affect the measurable $\mathbf{J}(t)$. The total change in bulk polarization in a time interval $[0, T]$ is also well defined as the integrated current: $\Delta\mathbf{P} = \int_0^T \mathbf{J}(t) dt$. It can be determined, apart from an integer multiple of the quantum, by evaluating $\mathbf{P}(t)$ at the end points: $\Delta\mathbf{P} = \mathbf{P}(T) - \mathbf{P}(0)$. In practice the remaining indeterminacy can be removed in the manner described in Ref. 1, by evaluating $\mathbf{P}(t)$ with sufficient frequency during that interval.

To establish Eqs. (20) and (21), we first evaluate $d\mathbf{P}/dt$ by taking the time derivative of Eq. (21) and obtain, after an integration by parts,

$$\frac{dP_\alpha}{dt} = -\frac{ie}{(2\pi)^3} \sum_{n=1}^M \int d\mathbf{k} [\langle \dot{v}_{\mathbf{k}n} | \partial_{k_\alpha} v_{\mathbf{k}n} \rangle - \text{c.c.}]. \quad (23)$$

Inserting the TDSE, Eq. (14), we note that the contribution arising from the second term therein, which explicitly involves \mathcal{E} , may be written as

$$\tilde{J}_\alpha = \frac{e^2}{(2\pi)^3 \hbar} \sum_{n=1}^M \sum_{\beta} \mathcal{E}_\beta \int d\mathbf{k} \Omega_{\alpha\beta}^{(n)}(\mathbf{k}), \quad (24)$$

where

$$\Omega_{\alpha\beta}^{(n)}(\mathbf{k}) = i[\langle \partial_{k_\alpha} v_{\mathbf{k}n} | \partial_{k_\beta} v_{\mathbf{k}n} \rangle - \langle \partial_{k_\beta} v_{\mathbf{k}n} | \partial_{k_\alpha} v_{\mathbf{k}n} \rangle]. \quad (25)$$

This takes the form of a (nonadiabatic) Berry curvature.¹⁹ Using Stokes’ theorem, its volume integral can be turned into a surface integral around the edges of the BZ of the Berry connection $\mathbf{A}_{\mathbf{k},nn}$, where

$$A_{\mathbf{k},nn}^\alpha = i \langle v_{\mathbf{k}n} | \partial_{k_\alpha} v_{\mathbf{k}n} \rangle. \quad (26)$$

Such an integral vanishes in a periodic gauge, so that $\tilde{J}_\alpha = 0$. The remaining contribution, arising from the insertion of the first term of Eq. (14) into Eq. (23), then gives

$$\frac{dP_\alpha}{dt} = \frac{e}{(2\pi)^3 \hbar} \sum_{n=1}^M \int d\mathbf{k} [\langle v_{\mathbf{k}n} | \hat{H}_{\mathbf{k}}^0 | \partial_{k_\alpha} v_{\mathbf{k}n} \rangle + \text{c.c.}]. \quad (27)$$

On the other hand, the current is

$$J_\alpha = -\frac{e}{v} \text{Tr}_c(\hat{n} \hat{v}_\alpha). \quad (28)$$

Here Tr_c denotes the trace per unit cell,

$$\text{Tr}_c(\hat{O}) = \frac{1}{N} \int \mathcal{O}(\mathbf{r}, \mathbf{r}) d\mathbf{r}, \quad (29)$$

where N is the (formally infinite) number of real-space cells in the system. The velocity operator is defined as

$$\hat{v}_\alpha = \frac{1}{i\hbar} [\hat{r}_\alpha, \hat{H}]. \quad (30)$$

Inserting the Hamiltonian (2) and using $[\hat{r}_\alpha, \hat{H}\mathcal{E}] = 0$,

$$\hat{v}_\alpha = \frac{1}{i\hbar} [\hat{r}_\alpha, \hat{H}^0]. \quad (31)$$

In the position representation we find, combining Eqs. (8), (28), and (31), invoking the lattice periodicity of the integrand to replace $(1/N) \int d\mathbf{r}$ by $\int_v d\mathbf{r}$, and inserting the identity $\hat{\mathbf{1}} = \int d\mathbf{r}' |\mathbf{r}'\rangle \langle \mathbf{r}'|$,

$$J_\alpha = -\frac{e}{(2\pi)^3 \hbar} \sum_{n=1}^M \int d\mathbf{k} \int_v d\mathbf{r} \int d\mathbf{r}' v_{\mathbf{k}n}^*(\mathbf{r}') v_{\mathbf{k}n}(\mathbf{r}) \times H^0(\mathbf{r}', \mathbf{r}) \partial_{k_\alpha} e^{-i\mathbf{k} \cdot (\mathbf{r}' - \mathbf{r})}. \quad (32)$$

Integrating by parts in k_α (the boundary term vanishes in a periodic gauge), and using

$$H_{\mathbf{k}}^0(\mathbf{r}', \mathbf{r}) = e^{-i\mathbf{k} \cdot (\mathbf{r}' - \mathbf{r})} H^0(\mathbf{r}', \mathbf{r}), \quad (33)$$

J_α reduces to exactly the same expression appearing on the right-hand side of Eq. (27). This completes the proof of Eqs. (20) and (21) for WR states evolving under the Hamiltonian (2).

We note in passing that the integral on the right-hand side of Eq. (27) can be recast as

$$\int d\mathbf{k} [\partial_{k_\alpha} \langle v_{\mathbf{k}n} | \hat{H}_{\mathbf{k}}^0 | v_{\mathbf{k}n} \rangle - \langle v_{\mathbf{k}n} | (\partial_{k_\alpha} \hat{H}_{\mathbf{k}}^0) | v_{\mathbf{k}n} \rangle]. \quad (34)$$

The first term vanishes in a periodic gauge, leading to the more familiar-looking form

$$J_\alpha = -\frac{e}{(2\pi)^3} \sum_{n=1}^M \int d\mathbf{k} \langle v_{\mathbf{k}n} | \hat{v}_\alpha(\mathbf{k}) | v_{\mathbf{k}n} \rangle, \quad (35)$$

where $\hat{v}_\alpha(\mathbf{k}) = (1/\hbar)(\partial_{k_\alpha} \hat{H}_\mathbf{k}^0)^{14}$

The above derivations (and indeed all the results in this paper) remain valid for nonlocal pseudopotentials such as those used in *ab initio* calculations, since the definition of the velocity as the commutator (30) remains valid for such pseudopotentials.

B. Discussion

It is remarkable that a knowledge of the wave functions at $t=0$ and $t=T$ is sufficient to infer, to within a factor of $(e/v)\mathbf{R}$, the net amount of current that flowed through the bulk in the intervening time. This is a direct consequence of representability by localized Wannier functions, that is, of the insulating-like character of the many-electron system. For such systems the integral in Eq. (22) can be evaluated, and it becomes possible to track the time evolution of the electronic center of mass, i.e., of \mathbf{P} . Indeed, the center of mass can be meaningfully defined within periodic boundary conditions only for many-electron states that are localized in the manner of insulating states.^{20,21} Under these conditions, the history of the coherent current flow is contained (modulo the quantum of polarization) in the initial and final wave functions, related by the time evolution operator $\exp[-(i/\hbar)\int_0^T \hat{H}(t)dt]$.

This result was previously established for adiabatic charge flow,¹ under the assumption that the ground state is separated from excited states by finite energy gaps everywhere in the BZ. In nonadiabatic situations the occupied manifold acquires a significant excited-state admixture, so that it becomes impossible to identify an energy gap. Instead, underlying the derivation in Sec. III A is a weaker assumption, namely, that the many-electron state has a localized nature, as reflected by the ability to construct, via Eq. (18), Wannier functions having a finite localization length.^{21,22} (Numerical calculations of the localization length will be presented in Sec. VI.) For instance, when taking k derivatives, we assumed a ‘‘differentiable gauge’’ for $|v_{\mathbf{k}n}\rangle$. This is only possible if the character of the electronic manifold changes slowly with \mathbf{k} , which is precisely what is measured by the localization length.³ These observations are in line with Kohn’s viewpoint that the defining feature of the insulating state is wave-function localization, not the existence of an energy gap.²⁰

IV. DYNAMICAL EQUATIONS

Having found the Berry-phase formula (21) for the dynamic polarization in the presence of a field $\mathcal{E}(t)$, let us now use it to obtain computationally tractable dynamical equations under the Hamiltonian (2). The starting point is the observation that the dipole term $\hat{H}^\mathcal{E}$ contributes $-v\mathbf{P}(t) \cdot \mathcal{E}(t)$ to the energy per unit cell. An energy functional valid for periodic boundary conditions is then obtained by expressing $\mathbf{P}(t)$ via the TBP formulas. This program was previously carried out for insulators in static fields,^{4,7-9} where stationary states were computed by minimizing that energy functional after applying a regularization procedure (truncation of the Wannier functions in real space or discretization of k space).

Our strategy for the time-dependent problem is to impose stationarity on the corresponding action functional. Following Refs. 7 and 8, we adopt here a k -space formulation, which is particularly well suited for numerical work. Special emphasis will be put on the discrete- k case since this is the relevant one for numerical implementations.

A. Continuum- k case

In the continuum- k limit the TDSE may be formally obtained from a Lagrangian density $\mathcal{L}(\mathbf{k})$ such that the Lagrangian per unit cell is $L = \Omega_B^{-1} \int d\mathbf{k} \mathcal{L}(\mathbf{k})$. For WR states under the Hamiltonian (2) we have

$$\mathcal{L}(\mathbf{k}) = i\hbar \sum_{n=1}^M \langle v_{\mathbf{k}n} | \dot{v}_{\mathbf{k}n} \rangle - E(\mathbf{k}), \quad (36)$$

where

$$E(\mathbf{k}) = \sum_{n=1}^M \langle v_{\mathbf{k}n} | \hat{H}_\mathbf{k}^0 + ie\mathcal{E} \cdot \partial_\mathbf{k} | v_{\mathbf{k}n} \rangle. \quad (37)$$

Using Eq. (21) and defining the zero-field energy functional

$$E^0 = \Omega_B^{-1} \sum_{n=1}^M \int d\mathbf{k} \langle v_{\mathbf{k}n} | \hat{H}_\mathbf{k}^0 | v_{\mathbf{k}n} \rangle, \quad (38)$$

one finds the total-energy functional

$$E = \Omega_B^{-1} \int d\mathbf{k} E(\mathbf{k}) = E^0 - v\mathbf{P} \cdot \mathcal{E}. \quad (39)$$

The Euler-Lagrange equation²³

$$\frac{d}{dt} \frac{\delta \mathcal{L}}{\delta \dot{v}_{\mathbf{k}n}} + \frac{d}{d\mathbf{k}} \frac{\delta \mathcal{L}}{\delta \partial_\mathbf{k} v_{\mathbf{k}n}} - \frac{\delta \mathcal{L}}{\delta v_{\mathbf{k}n}} = 0 \quad (40)$$

then leads to the dynamical equation (14).

As already mentioned, the choice of dynamical equation for $|v_{\mathbf{k}n}\rangle$ is not unique. An alternative to Eq. (14) is

$$i\hbar |\dot{v}_{\mathbf{k}n}\rangle = (\hat{H}_\mathbf{k}^0 + ie\mathcal{E} \cdot \tilde{\partial}_\mathbf{k}) |v_{\mathbf{k}n}\rangle. \quad (41)$$

The bare derivative $\partial_\mathbf{k}$ has been replaced by

$$\tilde{\partial}_\mathbf{k} = \partial_\mathbf{k} + i \sum_{m,n=1}^M \mathbf{A}_{\mathbf{k},mn} |v_{\mathbf{k}m}\rangle \langle v_{\mathbf{k}n}|, \quad (42)$$

where $\mathbf{A}_{\mathbf{k},mn}$ is given by Eq. (26). The operator $\tilde{\partial}_\mathbf{k}$ is a multi-band version of the covariant derivative²⁴ and is discussed further in Appendix B. Although the field-coupling term in Eq. (41) is no longer a scalar-potential term in the strict sense, we will continue to view it as such in a generalized sense.

Equation (41) preserves the orthonormality of the $|v_{\mathbf{k}n}\rangle$ and generates the correct dynamics for the density matrix. [These properties rely on $(A_\mathbf{k}^\alpha)^\dagger = A_\mathbf{k}^\alpha$, which follows from $\partial_{k_\alpha} \langle v_{\mathbf{k}n} | v_{\mathbf{k}m} \rangle = 0$.²⁵] The latter is most easily seen from the dynamics of the projector

$$\hat{P}_{\mathbf{k}} = \sum_{n=1}^M |v_{\mathbf{k}n}\rangle \langle v_{\mathbf{k}n}|, \quad (43)$$

which completely specifies the occupied subspace at \mathbf{k} while being insensitive to unitary rotations inside that subspace. After some algebra, it can be shown that while the individual $|v_{\mathbf{k}n}\rangle$ behave differently under Eqs. (14) and (41), $\hat{P}_{\mathbf{k}}$ stays the same.

An advantage of introducing Eq. (41) in place of Eq. (14) is that, upon the discretization of k space, the former leads to an evolution equation at point \mathbf{k} that is gauge covariant (in the sense of transforming in the obvious way under unitary rotations among occupied states at \mathbf{k} and being invariant under such rotations at neighboring points \mathbf{k}'), as will become clear in the following section.

B. Discrete- k case

This is the relevant case for numerical work. The Lagrangian for a uniform mesh of N points in the BZ is

$$L = \frac{i\hbar}{N} \sum_{n=1}^M \sum_{\mathbf{k}} \langle v_{\mathbf{k}n} | \dot{v}_{\mathbf{k}n} \rangle - E, \quad (44)$$

where E is the energy in an electric field,

$$E = E^0 - v \boldsymbol{\mathcal{E}} \cdot \mathbf{P}, \quad (45)$$

with

$$E^0 = \frac{1}{N} \sum_{n=1}^M \sum_{\mathbf{k}} \langle v_{\mathbf{k}n} | \hat{H}_{\mathbf{k}}^0 | v_{\mathbf{k}n} \rangle \quad (46)$$

and a discretized expression for \mathbf{P} to be given shortly. Applying the Lagrangian equations of motion²³

$$\frac{d}{dt} \frac{\delta L}{\delta \dot{v}_{\mathbf{k}n}} - \frac{\delta L}{\delta v_{\mathbf{k}n}} = 0 \quad (47)$$

yields

$$i\hbar \frac{d}{dt} |v_{\mathbf{k}n}\rangle = \hat{H}_{\mathbf{k}}^0 |v_{\mathbf{k}n}\rangle - Nv \boldsymbol{\mathcal{E}} \cdot \frac{\delta \mathbf{P}}{\delta v_{\mathbf{k}n}}. \quad (48)$$

Writing

$$\mathbf{P} = \frac{1}{2\pi} \sum_{i=1}^3 \mathbf{a}_i (\mathbf{P} \cdot \mathbf{b}_i), \quad (49)$$

where \mathbf{a}_i and \mathbf{b}_i are the direct and reciprocal lattice vectors, respectively, and defining

$$v \mathbf{P} \cdot \mathbf{b}_i = -e \bar{\Gamma}_i, \quad (50)$$

the last term in Eq. (48) becomes

$$+ \frac{Ne}{2\pi} \sum_{i=1}^3 (\boldsymbol{\mathcal{E}} \cdot \mathbf{a}_i) \frac{\delta \bar{\Gamma}_i}{\delta v_{\mathbf{k}n}}. \quad (51)$$

According to Ref. 1, $\bar{\Gamma}_i$ is the string-averaged discretized geometric phase along the \mathbf{b}_i direction,

$$\bar{\Gamma}_i = -\frac{1}{N_i^\perp} \sum_{l=1}^{N_i^\perp} \text{Im} \ln \prod_{j=0}^{N_i^\parallel-1} \det S(\mathbf{k}_j^{(i)}, \mathbf{k}_{j+1}^{(i)}). \quad (52)$$

Here $S_{mn}(\mathbf{k}, \mathbf{k}') = \langle v_{\mathbf{k}m} | v_{\mathbf{k}'n} \rangle$ is the $M \times M$ overlap matrix, N_1^\perp is the number of strings along \mathbf{b}_1 , each containing N_1^\parallel points $\mathbf{k}_j^{(1)} = \mathbf{k}_1^{(1)} + j\Delta\mathbf{k}_1$, $\mathbf{k}_1^{(1)}$ is a point on the $(\mathbf{b}_2, \mathbf{b}_3)$ plane labeled by l , and $\Delta\mathbf{k}_1 = \mathbf{b}_1 / N_1^\parallel$. Equations (50) and (52) provide the discretization of the nonadiabatic Berry-phase polarization, Eq. (21). [A discrete- k formula for the macroscopic current $\mathbf{J}(t)$ is given in Appendix D.] As in the continuum case, a periodic gauge is assumed.

A compact expression for $\delta \bar{\Gamma}_i / \langle \delta v_{\mathbf{k}n} |$ is derived in Appendix C 2 using the following notation. Let $\mathbf{k}i\sigma = \mathbf{k} + \sigma \Delta\mathbf{k}_i$, where $\sigma = \pm 1$. The overlap matrix becomes $S_{\mathbf{k}i\sigma, mn} = \langle v_{\mathbf{k}n} | v_{\mathbf{k}i\sigma, n} \rangle$. Next we define

$$|\tilde{v}_{\mathbf{k}i\sigma, n}\rangle = \sum_{m=1}^M (S_{\mathbf{k}i\sigma}^{-1})_{mn} |v_{\mathbf{k}i\sigma, m}\rangle, \quad (53)$$

which is a ‘‘dual’’ of $|v_{\mathbf{k}n}\rangle$ in the space of the $|v\rangle$'s at the neighboring point $\mathbf{k}i\sigma$, since

$$\langle v_{\mathbf{k}n} | \tilde{v}_{\mathbf{k}i\sigma, m} \rangle = \delta_{n,m}. \quad (54)$$

$|\tilde{v}_{\mathbf{k}i\sigma, n}\rangle$ are gauge covariant in the sense that (i) they are invariant under unitary rotations among $|v_{\mathbf{k}i\sigma, n}\rangle$ at any neighboring point $\mathbf{k}i\sigma$ and (ii) they transform under unitary rotations among $|v_{\mathbf{k}n}\rangle$ in the same manner as $|v_{\mathbf{k}n}\rangle$ themselves, i.e.,

$$|\tilde{v}_{\mathbf{k}i\sigma, n}\rangle \rightarrow \sum_{m=1}^M U_{\mathbf{k}, mn} |\tilde{v}_{\mathbf{k}i\sigma, m}\rangle. \quad (55)$$

Then it is shown in Appendix C2 that

$$\frac{\delta \bar{\Gamma}_i}{\langle \delta v_{\mathbf{k}n} |} = \frac{i}{2N_i^\perp} \sum_{\sigma=\pm 1} \sigma |\tilde{v}_{\mathbf{k}i\sigma, n}\rangle. \quad (56)$$

Combining Eqs. (48), (51), and (56), and defining

$$|w_{\mathbf{k}n}\rangle = \frac{ie}{4\pi} \sum_{i=1}^3 N_i^\parallel (\boldsymbol{\mathcal{E}} \cdot \mathbf{a}_i) \sum_{\sigma=\pm 1} \sigma |\tilde{v}_{\mathbf{k}i\sigma, n}\rangle, \quad (57)$$

the dynamical equation becomes

$$i\hbar \frac{d}{dt} |v_{\mathbf{k}n}\rangle = \hat{H}_{\mathbf{k}}^0 |v_{\mathbf{k}n}\rangle + |w_{\mathbf{k}n}\rangle. \quad (58)$$

Equation (58) is a discretized version of Eq. (41), i.e.,

$$|w_{\mathbf{k}n}\rangle \simeq ie \boldsymbol{\mathcal{E}} \cdot \tilde{\delta}_{\mathbf{k}} |v_{\mathbf{k}n}\rangle. \quad (59)$$

This is connected with the fact that the duals provide a natural framework for writing a finite-difference representation of $\tilde{\delta}_{\mathbf{k}} |v_{\mathbf{k}n}\rangle$.¹⁰ In our notation,

$$\Delta \mathbf{k}_i \cdot \tilde{\partial}_{\mathbf{k}} |v_{\mathbf{k}n}\rangle \simeq \frac{1}{2} \sum_{\sigma=\pm 1} \sigma |\tilde{v}_{\mathbf{k}i\sigma,n}\rangle. \quad (60)$$

Both dynamical equations (14) and (41) lead to $d\langle v_{\mathbf{k}n}|v_{\mathbf{k}n}\rangle/dt=0$ for WR manifolds, so that the time evolution of the individual states $|v_{\mathbf{k}n}\rangle$ is unitary. This property is preserved in the discretized form (58), since $\langle v_{\mathbf{k}n}|w_{\mathbf{k}n}\rangle=0$. In order to take advantage of certain unitary integration algorithms, it is useful to recast the term $|w_{\mathbf{k}n}\rangle$ on the right-hand side as a Hermitian operator acting on $|v_{\mathbf{k}n}\rangle$. For that purpose let us define

$$\hat{P}_{\mathbf{k}i\sigma} = \sum_{n=1}^M |\tilde{v}_{\mathbf{k}i\sigma,n}\rangle \langle v_{\mathbf{k}n}|, \quad (61)$$

which converts an occupied state at \mathbf{k} into its dual at $\mathbf{k}i\sigma$ and is invariant under gauge transformations (i.e., under independent unitary rotations among occupied states at both \mathbf{k} and $\mathbf{k}i\sigma$). It follows that the operator

$$\hat{w}_{\mathbf{k}}(\mathcal{E}) = \frac{ie}{4\pi} \sum_{i=1}^3 N_i^{\parallel}(\mathcal{E} \cdot \mathbf{a}_i) \sum_{\sigma} \sigma \hat{P}_{\mathbf{k}i\sigma} \quad (62)$$

turns $|v_{\mathbf{k}n}\rangle$ into $|w_{\mathbf{k}n}\rangle$, which is the property we seek. Lastly, for the purpose of acting on $|v_{\mathbf{k}n}\rangle$ the non-hermitian $\hat{w}_{\mathbf{k}}$ can be replaced by $\hat{w}_{\mathbf{k}} + \hat{w}_{\mathbf{k}}^{\dagger}$ since $\hat{P}_{\mathbf{k}}\hat{P}_{\mathbf{k}i\sigma} = \hat{P}_{\mathbf{k}}$, so that $\hat{Q}_{\mathbf{k}}\hat{w}_{\mathbf{k}} = \hat{w}_{\mathbf{k}}$ (where $\hat{Q}_{\mathbf{k}} = 1 - \hat{P}_{\mathbf{k}}$) and therefore $\hat{w}_{\mathbf{k}}^{\dagger}|v_{\mathbf{k}n}\rangle = 0$. We have thus achieved our goal: Eq. (58) now takes the canonical form of a TDSE,

$$i\hbar \frac{d}{dt} |v_{\mathbf{k}n}\rangle = \hat{T}_{\mathbf{k}} |v_{\mathbf{k}n}\rangle, \quad (63)$$

with a Hermitian operator on the right-hand side:

$$\hat{T}_{\mathbf{k}}(\mathcal{E}) = \hat{H}_{\mathbf{k}}^0 + \hat{w}_{\mathbf{k}}(\mathcal{E}) + \hat{w}_{\mathbf{k}}^{\dagger}(\mathcal{E}). \quad (64)$$

We remarked previously that in the continuum- k limit Eq. (58) reduces to Eq. (41). The corresponding analysis for Eqs. (63) and (64) is left to Appendix B.

The operator $\hat{w}_{\mathbf{k}}$ appearing in Eq. (64) is defined via Eqs. (53), (61), and (62). It should be emphasized that it depends explicitly on the occupied states at \mathbf{k} and $\mathbf{k}i\sigma$. In particular, even when $\hat{H}_{\mathbf{k}}^0$ and \mathcal{E} are time independent, if the occupied manifolds at \mathbf{k} and $\mathbf{k}i\sigma$ are changing over time, so is $\hat{T}_{\mathbf{k}}$. However, $\hat{T}_{\mathbf{k}}$ remains invariant under unitary rotations at k points \mathbf{k} and $\mathbf{k}i\sigma$. Hence the resulting dynamics of the occupied manifold [Eq. (66) below] has the essential property of being insensitive to the gauge arbitrariness that is always present in numerical simulations.

Note that when the Lagrangian procedure was applied in Sec. IV A to the continuum- k problem, we arrived at Eq. (14), which contains $\partial_{\mathbf{k}}|v_{\mathbf{k}n}\rangle$. When the same was done after discretization, the resulting dynamical equation contained instead $\tilde{\partial}_{\mathbf{k}}|v_{\mathbf{k}n}\rangle$. The reason is that the gradient of the discretized Berry's phase, Eq. (56), is by construction orthogonal to the occupied subspace at \mathbf{k} , whereas the corresponding continuum- k term used in Sec. IV A was not. Had we or-

thogonalized that term, we would have obtained $\hat{Q}_{\mathbf{k}}\partial_{\mathbf{k}}|v_{\mathbf{k}n}\rangle$ instead of $\partial_{\mathbf{k}}|v_{\mathbf{k}n}\rangle$, which is equivalent to $\tilde{\partial}_{\mathbf{k}}|v_{\mathbf{k}n}\rangle$ (see Appendix B).

C. Numerical time integration

In the applications of Sec. VI we use the algorithm²⁶

$$|v_{\mathbf{k}n}(t+\Delta t)\rangle = \frac{1 - i\hbar(\Delta t/2)\hat{T}_{\mathbf{k}}(t)}{1 + i\hbar(\Delta t/2)\hat{T}_{\mathbf{k}}(t)} |v_{\mathbf{k}n}(t)\rangle \quad (65)$$

to perform the time integration. Note that in order to use this algorithm it was necessary to invoke the form (63) of the TDSE. The Hermiticity of $\hat{T}_{\mathbf{k}}$ guarantees that the time evolution is strictly unitary for any value of Δt . Since the system under study in Sec. VI is a tight-binding model with only three basis orbitals, the matrix inversion is very inexpensive. The same algorithm has been successfully used to perform self-consistent time-dependent density-functional calculations of the optical properties of atomic clusters using localized orbitals as a basis set.⁴⁵ For calculations with large basis sets (e.g., plane waves) more efficient algorithms are available.^{27,28}

Owing to the Hermiticity of $\hat{T}_{\mathbf{k}}$, the projector (43) obeys

$$\frac{d\hat{P}_{\mathbf{k}}}{dt} = \frac{1}{i\hbar} [\hat{T}_{\mathbf{k}}, \hat{P}_{\mathbf{k}}]. \quad (66)$$

Hence, a variation of the above approach would be to replace $\hat{T}_{\mathbf{k}}$ by

$$\hat{\mathcal{T}}_{\mathbf{k}} = \hat{Q}_{\mathbf{k}}\hat{T}_{\mathbf{k}} + \hat{T}_{\mathbf{k}}\hat{Q}_{\mathbf{k}}, \quad (67)$$

which is also Hermitian. Because $[\hat{\mathcal{T}}_{\mathbf{k}}, \hat{P}_{\mathbf{k}}] = [\hat{T}_{\mathbf{k}}, \hat{P}_{\mathbf{k}}]$, this choice does not change the dynamics of the occupied subspace $\hat{P}_{\mathbf{k}}$, but it does change the dynamics of the individual states $|v_{\mathbf{k}n}\rangle$. In fact, $\hat{\mathcal{T}}_{\mathbf{k}}$ generates a *parallel transport* evolution characterized by $\langle v_{\mathbf{k}n}|\dot{v}_{\mathbf{k}n}\rangle = 0$, thus discarding the ‘‘irrelevant’’ part of the dynamics associated with phase factors and unitary rotations inside the occupied subspace. We have found empirically, however, that the use of $\hat{\mathcal{T}}_{\mathbf{k}}$ in Eq. (65) appears to result in a less stable numerical time evolution, and we have therefore chosen to retain the original $\hat{T}_{\mathbf{k}}$ dynamics in our practical implementation.

D. Discussion

It may seem surprising that a linear potential can be accommodated in a theoretical description of a periodic bulk system. A commonly held viewpoint is that a linear potential can be implemented within periodic boundary conditions only for the case of a finite system (molecule or cluster) in a supercell, in which case it becomes possible to introduce a sawtooth potential as long as its discontinuity is located in a region of negligible electron density. To the contrary, Eqs. (14), (41), and (63) demonstrate that it is perfectly permissible to insist on the usual periodic boundary conditions on the wave functions while allowing for nonperiodicity of the

potential. This can be done because the potential takes the special form of a sum of spatially periodic and linear contributions, relevant to a crystal in a homogeneous electric field. As shown in Sec. II A, the action of the nonperiodic Hamiltonian, Eq. (2), then preserves the lattice periodicity of the density matrix, which can therefore be represented by periodic wave functions.

Incidentally, we note that a sawtooth operator of sorts is “hiding” behind the TBP formulas. The Berry-phase polarization has been recast as the expectation value of a properly defined center-of-mass position operator of the many-electron periodic system.²¹ That operator, introduced by Kohn,²⁰ is a sawtooth, not in real space but in the configuration space of the many-body wave function. It can only be constructed for wave functions having a certain disconnectedness (localization) property in configuration space characteristic of the insulating state. This observation is closely related to the discussion in Sec. III B.

Finally, we mention that an alternative approach for introducing a linear potential into a periodic solid is via the CMR formalism.¹⁴ This approach is summarized in Appendix A, where the connection with our formalism is established. The CMR dynamical equations appear to be less convenient for computational work. However, the advantages of the present formulation came at the expense of generality, since our equations are restricted to the scattering-free dynamics of initially insulating systems.

V. STABLE STATIONARY SOLUTIONS

A. Formulation

Let us try to find, for a constant $\mathcal{E} \neq 0$, solutions to Eq. (63) for which the occupied manifold remains unchanged over time. A natural guess is the manifold spanned by M eigenstates of $\hat{T}_{\mathbf{k}}$ at each \mathbf{k} ,

$$\hat{T}_{\mathbf{k}}|v_{\mathbf{k}n}\rangle = E_{\mathbf{k}n}(\mathcal{E})|v_{\mathbf{k}n}\rangle. \quad (68)$$

Since $\hat{T}_{\mathbf{k}}$ depends on the occupied states at the neighboring k points, Eq. (68) must be solved self-consistently among all \mathbf{k} . If a solution exists, the corresponding $\hat{T}_{\mathbf{k}}$ and $\hat{P}_{\mathbf{k}}$ commute and, according to Eq. (66), $d\hat{P}_{\mathbf{k}}/dt=0$, i.e., the solution is stationary.

We are now ready to make contact with Refs. 8 and 9, where the energy functional E of Nunes and Gonze,⁷ Eq. (45), was minimized at fixed \mathcal{E} . A stationary point of E has zero gradient: $|G_{\mathbf{k}n}\rangle = \delta E / \langle \delta v_{\mathbf{k}n} | = 0$, where the functional derivative is taken in such a way that the gradient is orthogonal to the occupied space. In Appendix C2 it is shown that

$$|G_{\mathbf{k}n}\rangle = (1/N)\hat{Q}_{\mathbf{k}}\hat{T}_{\mathbf{k}}|v_{\mathbf{k}n}\rangle, \quad (69)$$

so that solutions of Eq. (68) obey $|G_{\mathbf{k}n}\rangle = 0$. Thus, stationary solutions of the dynamical equation are stationary points of E .

A Hessian stability analysis³⁰ shows that a necessary condition for a stationary point of E to be a minimum is that the M lowest-lying eigenstates of $\hat{T}_{\mathbf{k}}$ are chosen. Since doing so at $\mathcal{E}=0$ yields the ground state, at finite \mathcal{E} that procedure

yields a state that is adiabatically connected to it by slowly ramping up the field, keeping the system in a minimum of E . Such “polarized manifolds” have been discussed previously in a perturbative framework,^{29,31,32} treating \mathbf{k} as a continuous variable. In that limit the electric-field perturbation becomes singular. That is, even an arbitrary small field induces a current via Zener tunneling to higher bands, and the polarized manifolds are not stationary, but rather, are long-lived resonances. In other words, an infinite crystal in the presence of a static electric-field does not have a ground state. This is reflected in E losing its minima as soon as \mathcal{E} departs from zero.

Instead, for a discrete mesh of k points, arguments can be given^{7,8} suggesting that E loses its minima only when the field exceeds a critical value $\mathcal{E}_c(N)$ that decreases as the number N of k points increases; this is supported by numerical calculations.^{8,9} It follows from the preceding discussion that the minima of E below $\mathcal{E}_c(N)$ are stable stationary solutions of the dynamical equation. Conversely, above $\mathcal{E}_c(N)$ there are no such solutions.

These two regimes—below and above the critical field—will be explored numerically in Sec. VI C via time-dependent calculations. If one stays below $\mathcal{E}_c(N)$, the stationary solutions can be computed using time-independent methods, such as the diagonalization algorithm described next or the minimization methods of Refs. 8 and 9.

B. Diagonalization algorithm

We have in Eq. (68) the basis for an algebraic method of computing stationary states at finite \mathcal{E} on a uniform k -point mesh, for $|\mathcal{E}| < \mathcal{E}_c(N)$: loop over the k points; for each one select the M eigenstates of $\hat{T}_{\mathbf{k}}$ with the lowest eigenvalues; iterate until the procedure converges at all \mathbf{k} and the occupied subspace stabilizes (this will only happen below \mathcal{E}_c). Even in a tight-binding model without charge self-consistency, the set of Eqs. (68) has to be solved self-consistently throughout the BZ, since the operators $\hat{T}_{\mathbf{k}}$ couple neighboring k points via their dependence on the $|v_{\mathbf{k}n}\rangle$. One may choose to update $\hat{T}_{\mathbf{k}}$ either inside or outside the loop over \mathbf{k} ; the latter option renders the algorithm parallelizable over k points.

We have tested this scheme on the tight-binding model of Sec. VI, and confirm that it produces the same state as a direct steepest-descent or conjugate-gradients minimization of the functional E .⁸ This algorithm may be especially suited for implementation in certain total-energy codes that are based on iteratively diagonalizing the Kohn-Sham Hamiltonian expanded in a small basis set of local orbitals.³³

C. Discussion

Equation (68) is a discretization of the time-independent version of Eq. (41):

$$(\hat{H}_{\mathbf{k}}^0 + ie\mathcal{E} \cdot \vec{\partial}_{\mathbf{k}})|v_{\mathbf{k}n}\rangle = E_{\mathbf{k}n}(\mathcal{E})|v_{\mathbf{k}n}\rangle. \quad (70)$$

An analysis of the eigenvalues of this equation will serve as a guide for discussing those of Eq. (68). (For the present

purposes we will assume that the continuum form (70) has solutions for $\mathcal{E} \neq 0$.) As a result of the properties of the covariant derivative (Appendix B) $E_{\mathbf{k}n}(\mathcal{E})$ are invariant under diagonal gauge transformations $U_{\mathbf{k},mn} = e^{i\theta_{\mathbf{k}m}} \delta_{m,n}$. Upon multiplying on the left by $\langle v_{\mathbf{k}n} |$ the second term on the left-hand-side of Eq. (70) vanishes. Integrating over \mathbf{k} and summing over n , we then find

$$\Omega_B^{-1} \sum_{n=1}^M \int d\mathbf{k} E_{\mathbf{k}n}(\mathcal{E}) = E^0(\mathcal{E}) \geq E^0(\mathcal{E}=0), \quad (71)$$

where $E^0(\mathcal{E})$ is the zero-field energy functional (38) evaluated at the field-polarized stationary state, and the inequality follows from the variational principle. The same properties hold for the eigenvalues of the discretized form (68), which can be obtained by diagonalizing $\hat{H}_{\mathbf{k}}^0$ inside the occupied manifold. We have here the interesting situation that a minimum of the *total* energy E can be obtained by solving the eigenvalue equations (68) whose eigenvalues, summed over n and \mathbf{k} give instead the *zero-field* contribution E^0 . This can be traced back to Eq. (B2), which expresses the ‘‘parallel-transport-like’’ nature of the covariant derivative.

The above is to be compared with the time-independent version of Eq. (14),

$$(\hat{H}_{\mathbf{k}}^0 + ie\mathcal{E} \cdot \partial_{\mathbf{k}}) |v'_{\mathbf{k}n}\rangle = E'_{\mathbf{k}n}(\mathcal{E}) |v'_{\mathbf{k}n}\rangle. \quad (72)$$

Under a diagonal transformation $|v'_{\mathbf{k}n}\rangle \rightarrow e^{i\theta_{\mathbf{k}m}} |v'_{\mathbf{k}n}\rangle$ its eigenvalues change as $E'_{\mathbf{k}n}(\mathcal{E}) \rightarrow E'_{\mathbf{k}n}(\mathcal{E}) - e\mathcal{E} \cdot \partial_{\mathbf{k}} \theta_{\mathbf{k}n}$. The analog of Eq. (71) is

$$\Omega_B^{-1} \sum_{n=1}^M \int d\mathbf{k} E'_{\mathbf{k}n}(\mathcal{E}) = E^0(\mathcal{E}) - v\mathcal{E} \cdot \mathbf{P}(\mathcal{E}). \quad (73)$$

The quantity on the right-hand side is now the total energy E , which is invariant only modulo $e\mathcal{E} \cdot \mathbf{R}$.

Although the individual eigenstates of Eq. (70) are in general different from those of Eq. (72), the self-consistent solutions for all \mathbf{k} and n span the same space in both cases, i.e., they differ only by a gauge transformation. It is then a matter of convenience to choose which of the two equations to solve in practice. Our particular approach is to discretize Eq. (70) in a gauge-covariant manner and then solve the resulting equation (68).

VI. NUMERICAL RESULTS

A. Tight-binding model

We have applied our scheme to the one-dimensional tight-binding model of Ref. 4, a three-band Hamiltonian with three atoms per unit cell of length $a=1$ and one orbital per atom,

$$\hat{H}^0[\alpha] = \sum_j \{ \epsilon_j(\alpha) \hat{c}_j^\dagger \hat{c}_j + t[\hat{c}_j^\dagger \hat{c}_{j+1} + \text{H.c.}] \}, \quad (74)$$

with the site energy given by $\epsilon_{3m+l}(\alpha) = \Delta \cos(\alpha - \beta_l)$. Here m is the cell index, $l = \{-1, 0, 1\}$ is the site index, and $\beta_l = 2\pi l/3$. Before the Berry-phase polarization can be computed³⁴ (or an electric field applied to the system^{4,35}), the

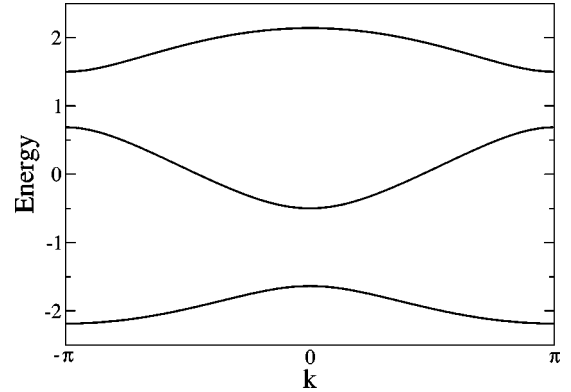


FIG. 1. Energy dispersion of the tight-binding model for the choice of parameters $t=1$, $\Delta=-1$, and $\alpha=0$.

position operator must be specified. Although this may be done without introducing additional parameters,³⁶ we adopt the simple prescription of Ref. 4: $\hat{x} = \sum_j x_j \hat{c}_j^\dagger \hat{c}_j$, with $x_j = j/3$. In the results reported below we have set $e = \hbar = 1$, $t=1$, and $\Delta=-1$, and only the lowest band is filled (with single occupancy). Figure 1 shows the band structure at zero field for $\alpha=0$.

B. Sliding charge-density wave

The Hamiltonian of Eq. (74) is a simple model of a commensurate charge-density wave which slides by one period as the parameter α evolves adiabatically through 2π . It is easiest to see this by noting that in the space of parameters $\Delta_x = \Delta \cos \alpha$ and $\Delta_y = \Delta \sin \alpha$, cycling α by 2π corresponds to tracing a circle about the origin in the Δ_x - Δ_y plane. The system is insulating (i.e., a gap remains open) at all points in this plane except for a singular point at the origin where the system is metallic. Thus, this cyclic adiabatic change in \hat{H}^0 takes the system along an insulating path that encircles this singular point, so that a quantized particle transport $\Delta P = \int_0^T J(t) dt$ of a unit charge is obtained.³⁷

Away from the adiabatic regime, deviations from exact quantization are expected. This can be understood from the fact that under nonadiabatic conditions the state at time t depends on the history at times $t' < t$. In particular, the final state may be different from the initial one even though $\hat{H}^0(T) = \hat{H}^0(0)$, in which case $P(T) - P(0) \neq 1$. By contrast, an adiabatically evolving system has no memory, being completely determined by the instantaneous $\hat{H}^0(t)$ and $d\hat{H}^0/dt$.

To illustrate this point, we increased α from 0 to 2π during a time interval $t \in [0, T]$ according to $\alpha(t) = 2\pi \sin^2(\pi t/2T)$, and held it constant afterwards. The system was prepared at $t=0$ in its ground state, and the wave functions evolved in time according to Eq. (65), using $\Delta t = 0.005$ (the same time step was used in all other simulations in this work). At each time step we computed the dynamic polarization using Eq. (52).

The resulting $P(t)$ for $T=80$ and 200 k points is shown in Fig. 2, where we also display the exact adiabatic ($T \rightarrow \infty$) limit $P_{\text{static}}[\alpha(t)]$ obtained by diagonalizing $\hat{H}_{\mathbf{k}}^0[\alpha(t)]$ on the

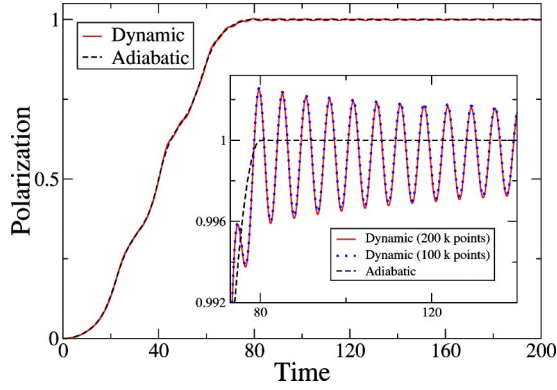


FIG. 2. (Color online) Time evolution of the polarization as a result of changing the sliding parameter α from 0 to 2π over the time interval $[0,80]$, using 200 k points. The solid line shows the actual dynamic polarization, while the dashed line shows the ground-state polarization of the instantaneous Hamiltonian. Inset: Detail of the remnant oscillations of the polarization after the Hamiltonian stops changing, at $t=80$. For comparison, the results using 100 k points are also shown.

same mesh of k points.³⁸ (To check that our calculations are converged with respect to the number of k points, the inset of Fig. 2 compares the results for 100 and 200 k points.) The dynamic polarization $P(t)$ obtained by solving the TDSE follows closely, but not exactly, the adiabatic curve. In particular, at the time $t=80$ when the Hamiltonian stops changing, the polarization differs slightly from unity (see inset in Fig. 2), indicating that the system is not in the ground state. The oscillations that follow arise from quantum interference (beats) between valence and conduction states, as a result of having excited electrons across the gap during $[0,T]$. Their period, of 5.5 time units, corresponds to the fundamental gap in Fig. 1, $E_{\text{gap}}=1.137$. This is consistent with the k -space distribution of the (small) electron-hole pair amplitude present in the system after time T : for a sliding period of $T=80$, the distribution is mostly concentrated around $k=0$, and it is essentially the lowest conduction band that gets populated. As the adiabatic limit is approached by increasing T , the amplitude of the remnant oscillations of the polarization decreases. This is illustrated in the upper panel of Fig. 3, where we compare $T=80$ with $T=120$.

Besides the macroscopic polarization $P(t)$, another quantity of interest is the electronic localization length $\xi(t)$ that characterizes the root-mean-square quantum fluctuations of the macroscopic polarization.²¹ It is given by $\xi^2=\Omega_1/M$, where Ω_1 is a gauge-invariant quantity which in one dimension is equal to the spread of the maximally localized Wannier functions (18).³ We have computed Ω_1 using Eq. (34) from Ref. 3, and in the lower panel of Fig. 3 we plot $\xi(t)$ against $\alpha(t)/2\pi$. In the adiabatic limit the resulting curve consists of three identical oscillations, reflecting the existence of three equivalent atoms in the unit cell. As nonadiabaticity increases, ξ tends to increase as well. Nevertheless, the electrons remain localized, i.e., insulatinglike, in the sense discussed in Sec. III B.³⁹

The above results are representative of the regime where deviations from adiabaticity are small. If we increase the

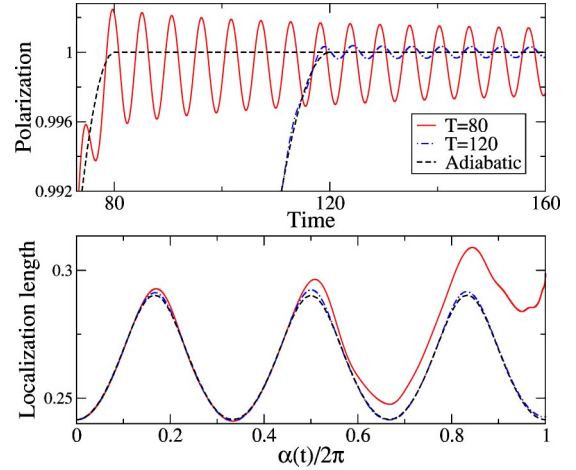


FIG. 3. (Color online) Upper panel: Same as Fig. 2, but now using two different time intervals, $[0,80]$ and $[0,120]$, for changing the sliding parameter α . Lower panel: electron localization length $\xi(t)$ vs the instantaneous value of α , during the time intervals $[0,T]$ over which α is changing.

degree of nonadiabaticity by choosing a smaller T (e.g., $T=40$), we begin to notice a linear increase of the polarization at later times. This new behavior can be traced to the excitation of electron and hole wave packets centered at some k_0 and propagating at different group velocities. Let ΔE_{k_0} be the interband separation, and Δv_g be the difference of group velocities of the two lowest bands, at k_0 . Then, in addition to the quantum beats of period $2\pi\hbar/\Delta E_{k_0}$ caused by the interband dynamics, we observe a linear-in- t term in $P(t)$ with slope proportional to Δv_g , reflecting the change in dipole moment as the electron-hole pair separates. [More precisely, the preceding statements apply only in the limit of a dense k -point mesh; for any finite mesh spacing Δk , the linear behavior is replaced by an oscillatory one with an amplitude scaling as $1/\Delta k$ and period $2\pi/(\Delta v_g \Delta k)$. Thus, an especially fine k -point mesh should be used if these effects are to be investigated.]

C. Gradual turn-on of an electric field

In the previous example the electric field was held at zero, and the dynamics was produced by varying the parameter α in \hat{H}^0 . Let us now study the polarization response of the system when an electric field $\mathcal{E}(t)$ is switched on linearly over a time interval $[0,T]$ and is held fixed afterwards. We have set $\alpha=0$, so that the ground state is centrosymmetric, with zero spontaneous polarization.

We begin by considering a situation where the final value of the field, \mathcal{E}_{max} , is smaller than the k -mesh-dependent critical field $\mathcal{E}_c(N)$ above which the energy functional (45) has no minima. This allows us to compare the dynamic polarization $P(t)$ with the static polarization $P_{\text{static}}[\mathcal{E}(t)]$ of the stationary state in the presence of the same field, which we find by minimizing the energy.⁸ In Fig. 4 we display the results for $\mathcal{E}_{\text{max}}=0.025$ and two different switching times $T=40$ and $T=80$. The simulation was done using 200 k points, to which corresponds a critical field $\mathcal{E}_c(N=200)\sim 0.037$. (The

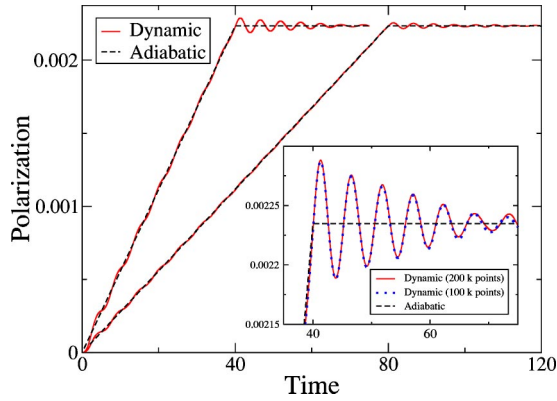


FIG. 4. (Color online) Time evolution of the polarization as a result of increasing the electric field from 0 to $\mathcal{E}_{\max}=0.025$ over two time intervals, $[0,40]$ and $[80,120]$, using 200 k points. The solid line shows the actual dynamic polarization, while the dashed line shows the static polarization for the instantaneous value of the field. Inset: Comparison of the dynamic polarization for 100 and 200 k points.

inset shows the agreement between the results obtained using 100 and 200 k points.) Clearly, $P(t)$ tracks quite closely the adiabatic curve $P_{\text{static}}[\mathcal{E}(t)]$, the more so as T increases. This illustrates the point, emphasized in Ref. 4, that the state obtained by minimizing a field-dependent energy functional should be thought of as the one which is generated from the zero-field state by adiabatically turning on \mathcal{E} .

Let us now explore the regime above $\mathcal{E}_c(N)$, where energy-minimization schemes fail. For $\mathcal{E}_{\max} > \mathcal{E}_c(N)$ the exact adiabatic limit of the process of ramping up the field is unattainable. Nevertheless, if \mathcal{E}_{\max} is small compared to the field scale at which *intrinsic* breakdown occurs (i.e., at which the Zener tunneling rate becomes of the order of interband frequencies, which is a bulk property⁴⁰), a *quasistationary* state should be reachable by turning on the field at a rate that is slow compared to the usual electronic processes, but fast compared to the characteristic tunneling time at the maximum field encountered. After the rampup is completed, but at times still short compared to the tunneling rate, this state should provide the appropriate extrapolation to fields above $\mathcal{E}_c(N)$ of the truly stationary state that exists below $\mathcal{E}_c(N)$.

To illustrate this situation, we repeated the calculation with 200 k points depicted in Fig. 4, but increasing the maximum field from 0.025 to 0.05, somewhat larger than $\mathcal{E}_c(200) \sim 0.037$. The resulting curve for $P(t)$ is very similar to that in Fig. 4, without any sign of runaway behavior. As a more striking example, we show in Fig. 5 the outcome of calculations with the same final field of $\mathcal{E}_{\max}=0.05$, but with even denser sets of 400 and 800 k points. For the latter $\mathcal{E}_c \sim 0.01$, considerably smaller than \mathcal{E}_{\max} , and still there is no sign of instability. (Note also that the $P(t)$ curve in Fig. 5—whose vertical scale differs from that in Fig. 4 by the same factor of 2 that exists between the respective values of \mathcal{E}_{\max} —looks almost identical to that in Fig. 4.) These results confirm that, as long as we are solving a *time-dependent* Schrödinger equation for a given history of switching on the field, there is no such thing as a Δk -dependent critical field; the thermodynamic limit of an infinitely dense k -point mesh is perfectly well defined. The only breakdown behavior that

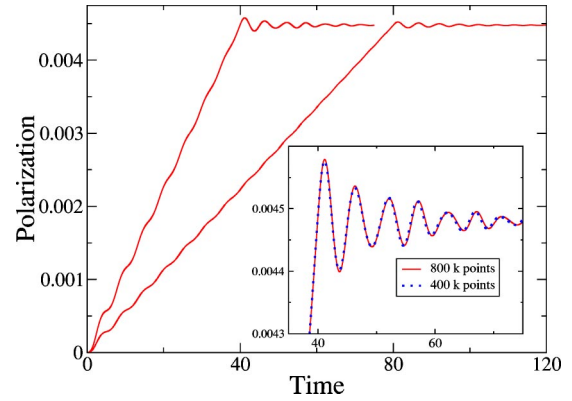


FIG. 5. (Color online) Same as Fig. 4, but now using $\mathcal{E}_{\max}=0.05$ and 800 k points. Since \mathcal{E}_{\max} is larger than the critical field for this number of k points ($\mathcal{E}_c \sim 0.01$), no adiabatic curve $P_{\text{static}}[\mathcal{E}(t)]$ is shown. Inset: Comparison of the dynamic polarization for 400 and 800 k points.

may be observed in short time scales is the physical one that occurs when the applied field is large enough such that the Zener tunneling rate becomes significant.^{41,40} The concept of a Δk -dependent critical field applies only to the attempt to obtain solutions in the presence of a static electric field from an energy variational principle. By going back to the original dynamical problem of slowly ramping up the field, we circumvent the difficulties that ultimately resulted from trying to treat as a (stable) stationary state what is really a long-lived resonance.

D. Dielectric function in a static field

There is great interest in modulating the optical properties of crystals and superlattices by applying static electric fields. An example of such an electro-optical effect is the field-induced modification of the dielectric function. This is known as the Franz-Keldysh effect, or electroabsorption. Although it has been extensively studied in bulk semiconductors,⁴² quantum wells,⁴³ and superlattices,⁴⁴ we are not aware of any first-principles investigations. The present method may provide a route to such calculations.

We compute the dielectric function in the presence of a static field \mathcal{E}_0 as follows. The system is prepared at $t=0$ in the stationary state polarized by a field $\mathcal{E}_0 + \Delta\mathcal{E}$, with $|\Delta\mathcal{E}| \ll |\mathcal{E}_0|$. By using a field of magnitude below the critical field, we are able to find that state by minimizing the energy. For $t > 0$ we let the system evolve in time in the presence of the target field \mathcal{E}_0 . Let $P_{\text{static}}[\mathcal{E}_0]$ be static polarization of the system under the field \mathcal{E}_0 . The polarization response to the step-function discontinuity in $\mathcal{E}(t) = \mathcal{E}_0 + \Delta\mathcal{E}\theta(-t)$ is $\Delta P(t) = P(t) - P_{\text{static}}[\mathcal{E}_0]$. To obtain the frequency-dependent response we need the Fourier transform of $\Delta P(t)$ for $t > 0$ only:

$$\Delta P(\omega) = \int_0^{+\infty} \Delta P(t) e^{(i\omega - \delta)t} dt, \quad (75)$$

where a damping factor δ has been introduced as an approximate way to account for level broadening.⁴⁵ To linear order in $\Delta\mathcal{E}$ the susceptibility is

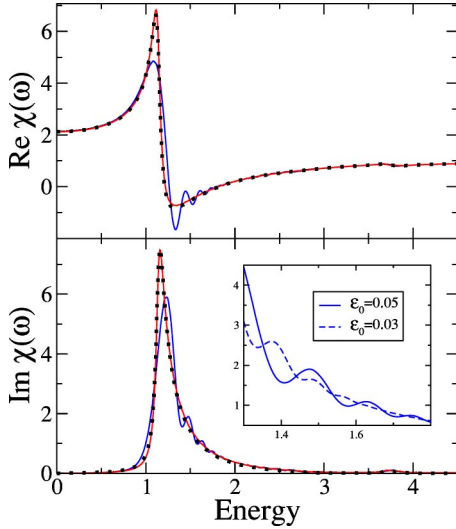


FIG. 6. (Color online) Susceptibility $\chi^{[\varepsilon_0]}(\omega)$ in the presence of a static field ε_0 , for $\alpha=0$ and 100 k points, using a level broadening $\delta=0.04$. Dotted lines: Kubo formula result for $\varepsilon_0=0$; solid lines: results using our method, for both $\varepsilon_0=0$ and $\varepsilon_0=0.05$. The latter displays the Franz-Keldysh effect. The inset compares the Franz-Keldysh oscillations for two different bias fields, $\varepsilon_0=0.05$ and $\varepsilon_0=0.03$.

$$\text{Re } \chi^{[\varepsilon_0]}(\omega) = \left. \frac{dP_{\text{static}}[\mathcal{E}]}{d\mathcal{E}} \right|_{\varepsilon=\varepsilon_0} - \frac{\omega}{\Delta\mathcal{E}} \text{Im } \Delta P(\omega), \quad (76)$$

$$\text{Im } \chi^{[\varepsilon_0]}(\omega) = \frac{\omega}{\Delta\mathcal{E}} \text{Re } \Delta P(\omega). \quad (77)$$

With this real-time approach the need to perform a summation over conduction-band states is circumvented. Previous real-time, scalar-potential approaches^{45,46} were restricted to finite systems, since it was unclear how to evaluate the dynamic macroscopic polarization of an extended system. A real-time, vector-potential scheme valid for bulk systems was proposed in Ref. 47.

We validate our method by comparing in Fig. 6 the ground-state susceptibility with the analytic Kubo formula (sum-over-states) result, using in both cases the same broadening δ and k -point mesh. Also shown in Fig. 6 is the susceptibility in the presence of a $\varepsilon_0=0.05$ bias field, displaying the Franz-Keldysh effect: an absorption tail below the gap caused by photon-assisted tunneling and oscillations above the gap.⁴² The Franz-Keldysh oscillations become more widely spaced with increasing ε_0 . This is illustrated in the inset of Fig. 6, where we compare them for $\varepsilon_0=0.05$ and $\varepsilon_0=0.03$.

VII. SUMMARY

The work of King-Smith and Vanderbilt demonstrated that the bulk electronic polarization, defined in terms of the current flowing during the *adiabatic* evolution of an insulating system in a *vanishing macroscopic electric field*, could be related to a Berry's phase defined over the manifold of occupied Bloch states.¹ We have generalized this result by con-

sidering the time evolution of an initially insulating electron system under the very general Hamiltonian (2), where the lattice-periodic part $\hat{H}^0(t)$ and the homogeneous electric field $\mathcal{E}(t)$ may have an arbitrarily strong and rapid variation in time. In the absence of scattering, we have proved that the integrated current $\Delta\mathbf{P}=\int\mathbf{J}(t)dt$ is still given by the King-Smith–Vanderbilt formula, but written in terms of the instantaneous Bloch-like solutions of the time-dependent Schrödinger equation. The coherent dynamic polarization $\mathbf{P}(t)$ was interpreted as a nonadiabatic geometric phase.¹⁸ These generalizations of the theory allowed us to justify recent developments in which the energy functional of Nunes and Gonze⁷ has been used as the basis for direct density-functional theory calculations of insulators in a static homogeneous electric field.^{8,9} The limitation of those methods to fields of magnitude smaller than a $\Delta\mathbf{k}$ -dependent critical field that vanishes in the thermodynamic limit has been removed: we have shown numerically that quasistationary states in finite fields exist for arbitrarily dense k -point meshes, and can be obtained by solving the time-dependent Schrödinger equation. The present method also provides a convenient framework for the computation of coherent time-dependent excitations in insulators. As an example, the dielectric function was calculated for a tight-binding model by considering the response to a step-function discontinuity in $\mathcal{E}(t)$, illustrating effects such as photon-assisted tunneling and Franz-Keldysh oscillations. A full *ab initio* implementation within the framework of time-dependent density-functional theory should be possible.

ACKNOWLEDGMENTS

This work was supported by NSF Grant No. DMR-0233925 and by DARPA/ONR Grant No. N00014-01-1-1061. We wish to thank M. H. Cohen for many useful discussions.

APPENDIX A: CRYSTAL-MOMENTUM REPRESENTATION

The introduction of linear scalar potentials in crystals is usually discussed in the language of the crystal-momentum representation (CMR).¹⁴ Instead, we have used the Berry-phase theory of polarization, and the purpose of this appendix is to show how to switch from one to the other. The CMR uses as a basis the eigenstates $|\psi_{\mathbf{k}m}\rangle$ of \hat{H}^0 with eigenvalues $E_{\mathbf{k}m}$. In accordance with Eq. (17) we assume that $|\psi_{\mathbf{k}m}(\mathbf{r})|^2$ integrates to one over the unit cell volume v . That implies^{48,49}

$$\langle\psi_{\mathbf{k}m}|\psi_{\mathbf{k}'l}\rangle\equiv\int\psi_{\mathbf{k}m}^*(\mathbf{r})\psi_{\mathbf{k}'l}(\mathbf{r})d\mathbf{r}=\Omega_B\delta(\mathbf{k}-\mathbf{k}')\delta_{ml}. \quad (\text{A1})$$

The CMR expansion of the identity operator is

$$\hat{1}=\Omega_B^{-1}\sum_{m=1}^{\infty}\int d\mathbf{k}|\psi_{\mathbf{k}m}\rangle\langle\psi_{\mathbf{k}m}|, \quad (\text{A2})$$

so that a general one-electron state $|\phi\rangle$ is expanded as

$$|\phi\rangle = \hat{\mathbf{1}}|\phi\rangle = \sum_{m=1}^{\infty} \int d\mathbf{k}' f_{\mathbf{k}'m} |\psi_{\mathbf{k}'m}\rangle, \quad (\text{A3})$$

where $f_{\mathbf{k}'m} = \Omega_B^{-1} \langle \psi_{\mathbf{k}'m} | \phi \rangle$. For the occupied Bloch-like states $|\phi_{\mathbf{k}n}\rangle$ in a WR manifold, the CMR wave function $f_{\mathbf{k}'m}(\mathbf{k}, n)$ takes the form

$$f_{\mathbf{k}'m}(\mathbf{k}, n) = c_{\mathbf{k}',nm} \delta(\mathbf{k}' - \mathbf{k}) \quad (\text{A4})$$

with $\sum_{m=1}^{\infty} |c_{\mathbf{k},nm}|^2 = 1$, which leads to Eq. (9).

1. Current and the CMR velocity operator

The velocity operator (31) is diagonal in \mathbf{k} and is conveniently split into a sum of two operators, one diagonal and the other off-diagonal in the band index:¹⁴

$$\hat{\mathbf{v}} = \hat{\mathbf{v}}^d + \hat{\mathbf{v}}^{\text{od}}. \quad (\text{A5})$$

The matrix elements of $\hat{\mathbf{v}}^d$ are

$$\langle \psi_{\mathbf{k}m} | \hat{\mathbf{v}}^d | \psi_{\mathbf{k}'l} \rangle = \Omega_B \delta(\mathbf{k} - \mathbf{k}') \delta_{ml} \mathbf{v}_{\mathbf{k}m}^d, \quad (\text{A6})$$

where

$$\mathbf{v}_{\mathbf{k}m}^d = \frac{1}{\hbar} \partial_{\mathbf{k}} E_{\mathbf{k}m}. \quad (\text{A7})$$

The matrix elements of $\hat{\mathbf{v}}^{\text{od}}$ are

$$\langle \psi_{\mathbf{k}m} | \hat{\mathbf{v}}^{\text{od}} | \psi_{\mathbf{k}'l} \rangle = \Omega_B \delta(\mathbf{k} - \mathbf{k}') \mathbf{v}_{\mathbf{k},ml}^{\text{od}}, \quad (\text{A8})$$

where

$$\mathbf{v}_{\mathbf{k},ml}^{\text{od}} = \frac{i}{\hbar} \mathbf{X}_{\mathbf{k},ml} [E_{\mathbf{k}m} - E_{\mathbf{k}l}] \quad (\text{A9})$$

and we have defined the Hermitian matrix

$$X_{\mathbf{k},ml}^{\alpha} = i \langle u_{\mathbf{k}m} | \partial_{k_{\alpha}} u_{\mathbf{k}l} \rangle, \quad (\text{A10})$$

which is analogous to Eq. (26) for the $|v_{\mathbf{k}n}\rangle$.

The current, Eq. (28), is split into intraband and interband parts,

$$\mathbf{J}(t) = \mathbf{J}_{\text{intra}}(t) + \mathbf{J}_{\text{inter}}(t). \quad (\text{A11})$$

Writing the density matrix as

$$\langle \psi_{\mathbf{k}m} | \hat{n} | \psi_{\mathbf{k}'l} \rangle = \Omega_B \delta(\mathbf{k} - \mathbf{k}') n_{\mathbf{k},ml}, \quad (\text{A12})$$

where

$$n_{\mathbf{k},ml} = \sum_{n=1}^M c_{\mathbf{k},nm} [c_{\mathbf{k},nl}]^*, \quad (\text{A13})$$

we find

$$\mathbf{J}_{\text{intra}} = -\frac{e}{v} \text{Tr}_c(\hat{n} \hat{\mathbf{v}}^d) = \frac{-e}{(2\pi)^3} \sum_{m=1}^{\infty} \int d\mathbf{k} n_{\mathbf{k},mm} \mathbf{v}_{\mathbf{k}m}^d \quad (\text{A14})$$

and

$$\mathbf{J}_{\text{inter}} = -\frac{e}{v} \text{Tr}_c(\hat{n} \hat{\mathbf{v}}^{\text{od}}) = \frac{-e}{(2\pi)^3} \sum_{m,l=1}^{\infty} \int d\mathbf{k} n_{\mathbf{k},ml} \mathbf{v}_{\mathbf{k},lm}^{\text{od}}. \quad (\text{A15})$$

In the above we used the CMR form of Eq. (29),

$$\text{Tr}_c(\hat{\mathcal{O}}) = \Omega_B^{-1} \sum_{m=1}^{\infty} \int d\mathbf{k} \frac{1}{N} \langle \psi_{\mathbf{k}m} | \hat{\mathcal{O}} | \psi_{\mathbf{k}m} \rangle, \quad (\text{A16})$$

where N should be taken to signify $\Omega_B \delta(0)$.⁴⁹

Plugging Eq. (9) into Eq. (27) yields, after some manipulations, Eqs. (A11), (A14), and (A15), confirming that the Berry-phase polarization correctly accounts for both intraband and interband contributions. It is instructive to consider some particular cases. The adiabatic current $\mathbf{J} = (d\mathbf{P}/d\lambda)\dot{\lambda}$ discussed in Refs. 1 and 37 is purely interband. If the perturbation is a sinusoidal electric field, the linear response is again a purely interband current, while the nonlinear response has also an intraband component.^{50,51}

2. Polarization and the CMR position operator

Along the same lines, one can show that the Berry-phase expression for \mathbf{P} is consistent with the CMR position operator, which takes the form¹⁴

$$\langle \psi_{\mathbf{k}m} | \hat{\mathbf{r}} | \psi_{\mathbf{k}'l} \rangle = -i\Omega_B \partial_{\mathbf{k}'} \delta(\mathbf{k}' - \mathbf{k}) \delta_{ml} + \Omega_B \delta(\mathbf{k}' - \mathbf{k}) \mathbf{X}_{\mathbf{k},ml}. \quad (\text{A17})$$

Combined with Eqs. (A12) and (A16) this yields

$$\mathbf{P} = -\frac{e}{v} \text{Tr}_c(\hat{n} \hat{\mathbf{r}}) = \frac{-e}{(2\pi)^3} \sum_{m,l=1}^{\infty} \int d\mathbf{k} n_{\mathbf{k},ml} \mathbf{X}_{\mathbf{k},lm}, \quad (\text{A18})$$

which is the same result one gets from inserting the CMR expansion (9) into the nonadiabatic Berry-phase formula (21). The linear character of $\hat{\mathbf{r}}$ is reflected in the above equation being defined only up to a quantum of polarization.

3. CMR dynamical equations

In the case where \hat{H}^0 (and hence the CMR basis) is constant in time, plugging Eq. (9) into the TDSE (14) yields the CMR form of the Schrödinger equation,^{32,52}

$$i\hbar \dot{c}_{\mathbf{k}m} = (E_{\mathbf{k}m} + ie \mathcal{E} \cdot \mathcal{D}_{\mathbf{k}}) c_{\mathbf{k}m}, \quad (\text{A19})$$

where we have simplified $c_{\mathbf{k},nm}$ to $c_{\mathbf{k}m}$ and defined

$$\mathcal{D}_{\mathbf{k}} c_{\mathbf{k}m} = \partial_{\mathbf{k}} c_{\mathbf{k}m} - i \sum_{l=1}^{\infty} \mathbf{X}_{\mathbf{k}l} c_{\mathbf{k}l}, \quad (\text{A20})$$

which is reminiscent of the covariant derivative, Eq. (42) (but note the difference in the sign of the last term). It is customary to write Eq. (A19) as

$$i\hbar \dot{c}_{\mathbf{k}m} = (E_{\mathbf{k}m}^{(1)} + ie \mathcal{E} \cdot \partial_{\mathbf{k}}) c_{\mathbf{k}m} + e \mathcal{E} \cdot \sum_{l \neq m}^{\infty} c_{\mathbf{k}l} \mathbf{X}_{\mathbf{k},ml}, \quad (\text{A21})$$

where

$$E_{\mathbf{k}m}^{(1)} = E_{\mathbf{k}m} + e\boldsymbol{\mathcal{E}} \cdot \mathbf{X}_{\mathbf{k},mm} \quad (\text{A22})$$

is a shifted energy eigenvalue. $E_{\mathbf{k}m}^{(1)}$ is identical to Eq. (37) except that $|v_{\mathbf{k}m}\rangle$ has been replaced by the zero-field eigenstate $|u_{\mathbf{k}m}\rangle$. Upon averaging over \mathbf{k} the last term on the right-hand side becomes the first-order shift in total energy, $-v\mathbf{P}_0 \cdot \boldsymbol{\mathcal{E}}$, where \mathbf{P}_0 is the spontaneous Berry-phase polarization.

In general the above TDSE has no stationary solutions. Approximate solutions—the Wannier-Stark states—result from restricting the wave-packet dynamics to a single band (the semiclassical approximation). That is achieved by dropping the sum on the right-hand side of Eq. (A21), which is responsible for interband tunneling.^{41,52}

Finally, combining Eqs. (A13) and (A19) produces the dynamical equation for the CMR density matrix:

$$i\hbar \dot{n}_{\mathbf{k},nm} = (E_{\mathbf{k}n} - E_{\mathbf{k}m})n_{\mathbf{k},nm} + ie\boldsymbol{\mathcal{E}} \cdot \partial_{\mathbf{k}} n_{\mathbf{k},nm} - e\boldsymbol{\mathcal{E}} \cdot \sum_{l=1}^{\infty} (n_{\mathbf{k},nl}\mathbf{X}_{\mathbf{k},lm} - \mathbf{X}_{\mathbf{k},nl}n_{\mathbf{k},lm}). \quad (\text{A23})$$

A closely related form has been used to study the nonlinear optical susceptibilities of semiconductors.^{51,53}

APPENDIX B: COVARIANT DERIVATIVE AND RELATED OPERATORS

In Sec. IV A we introduced a modified TDSE that contains the multiband covariant derivative $\tilde{\partial}_{\mathbf{k}}$, Eq. (42), that was instrumental for making contact with the discrete- k dynamical equations of Sec. IV B. Here we summarize the properties of the covariant derivative and other closely related operators.

The covariant derivative $\tilde{\partial}_{\mathbf{k}}|v_{\mathbf{k}n}\rangle$ of an occupied state transforms in the same way as that state under a gauge transformation, Eq. (10):

$$\tilde{\partial}_{\mathbf{k}}|v_{\mathbf{k}n}\rangle \rightarrow \sum_{m=1}^M U_{\mathbf{k},mn} \tilde{\partial}_{\mathbf{k}}|v_{\mathbf{k}m}\rangle. \quad (\text{B1})$$

Moreover, it is orthogonal to the occupied subspace at \mathbf{k} ,

$$\langle v_{\mathbf{k}m} | \tilde{\partial}_{\mathbf{k}} v_{\mathbf{k}n} \rangle = 0. \quad (\text{B2})$$

Recalling that parallel transport is characterized by $\langle v_{\mathbf{k}n} | \partial_{\mathbf{k}} v_{\mathbf{k}n} \rangle = 0$, for $m=n$ this relation shows that $\tilde{\partial}_{\mathbf{k}}$ acting in an arbitrary gauge gives the same result as $\partial_{\mathbf{k}}$ acting in the parallel-transport gauge that shares the same states at \mathbf{k} . In the discretized form (60) the property (B1) is a consequence of Eq. (55), and the property (B2) is a consequence of Eq. (54). Like $i\partial_{\mathbf{k}}$, $i\tilde{\partial}_{\mathbf{k}}$ is Hermitian. By this we mean that its matrix representation in an orthonormal basis (e.g., $|v_{\mathbf{k}n}\rangle$, $n=1, \dots, M$ complemented by a set of unoccupied states $|c_{\mathbf{k}j}\rangle$) is Hermitian. This is closely related to the hermiticity of the matrix $A_{\mathbf{k}}^{\alpha}$ defined in Eq. (26). Finally, note that

$$i\tilde{\partial}_{\mathbf{k}}|v_{\mathbf{k}n}\rangle = i\hat{Q}_{\mathbf{k}}\partial_{\mathbf{k}}|v_{\mathbf{k}n}\rangle = i\hat{Q}_{\mathbf{k}}\partial_{\mathbf{k}}\hat{P}_{\mathbf{k}}|v_{\mathbf{k}n}\rangle, \quad (\text{B3})$$

i.e., the action of $i\tilde{\partial}_{\mathbf{k}}$ on an occupied state is identical to that of $i\hat{Q}_{\mathbf{k}}\partial_{\mathbf{k}}$ and $i\hat{Q}_{\mathbf{k}}\partial_{\mathbf{k}}\hat{P}_{\mathbf{k}}$. They differ in how they act on the unoccupied states. Unlike $i\tilde{\partial}_{\mathbf{k}}$, the other two are not Hermitian: for instance, $(i\hat{Q}_{\mathbf{k}}\partial_{\mathbf{k}}\hat{P}_{\mathbf{k}})^{\dagger}|v_{\mathbf{k}n}\rangle = 0$. It follows from these considerations that Eq. (41) can be recast as

$$i\hbar|\dot{v}_{\mathbf{k}n}\rangle = [\hat{H}_{\mathbf{k}}^0 + e\boldsymbol{\mathcal{E}} \cdot (i\hat{Q}_{\mathbf{k}}\partial_{\mathbf{k}}\hat{P}_{\mathbf{k}} + \text{H.c.})]|v_{\mathbf{k}n}\rangle. \quad (\text{B4})$$

This is the form of the TDSE to which Eqs. (63) and (64) reduce in the continuum- k limit, since

$$\hat{w}_{\mathbf{k}} \approx ie\boldsymbol{\mathcal{E}} \cdot \hat{Q}_{\mathbf{k}}\partial_{\mathbf{k}}\hat{P}_{\mathbf{k}} \quad (\text{B5})$$

[compare with Eq. (59)].

APPENDIX C: GRADIENT OF THE ENERGY FUNCTIONAL

The purpose of this appendix is to obtain expressions for the derivatives of the two terms in the energy functional of Eq. (45) with respect to the occupied Bloch-like states in the discrete- k case. The results have been used in Secs. IV B and V A for the discussion of the time-dependent evolution equations and the stationary solutions, respectively.

1. Band-structure contribution

To find the gradient $\delta E / \langle \delta v_{\mathbf{k}n} |$ of the energy functional (45), let us isolate the terms that depend on $\langle v_{\mathbf{k}n} |$. Using Eq. (43) the zero-field part (46) can be expressed as $E^0 = (1/N)\sum_{\mathbf{k}} \text{tr}[\hat{P}_{\mathbf{k}}\hat{H}_{\mathbf{k}}^0]$, so that

$$\frac{\delta E^0}{\langle \delta v_{\mathbf{k}n} |} = \frac{1}{N} \frac{\delta \text{tr}[\hat{P}_{\mathbf{k}}\hat{H}_{\mathbf{k}}^0]}{\langle \delta v_{\mathbf{k}n} |}. \quad (\text{C1})$$

In order to allow for arbitrary variations of $\langle v_{\mathbf{k}n} |$, even those for which $\langle v_{\mathbf{k}n} |$ do not remain orthonormal, we write

$$\hat{P}_{\mathbf{k}} = \sum_{m,n=1}^M (\mathcal{S}_{\mathbf{k}}^{-1})_{mn} |v_{\mathbf{k}m}\rangle \langle v_{\mathbf{k}n}|, \quad (\text{C2})$$

where $\mathcal{S}_{\mathbf{k},mn} = \langle v_{\mathbf{k}m} | v_{\mathbf{k}n} \rangle$. Dropping the subscript \mathbf{k} ,

$$\begin{aligned} \delta \text{tr}[\hat{P}\hat{H}^0] &= \text{tr}[(\delta\hat{P})\hat{H}^0] \\ &= \sum_{m,n} (\mathcal{S}^{-1})_{mn} [\langle v_n | \hat{H}^0 | \delta v_m \rangle + \langle \delta v_n | \hat{H}^0 | v_m \rangle] \\ &\quad + \sum_{m,n} \langle v_n | \hat{H}^0 | v_m \rangle \delta(\mathcal{S}^{-1})_{mn}. \end{aligned} \quad (\text{C3})$$

Using $\delta(\mathcal{S}^{-1}) = -\mathcal{S}^{-2}\delta\mathcal{S}$ and $\delta\mathcal{S}_{mn} = \langle v_m | \delta v_n \rangle + \langle \delta v_m | v_n \rangle$, and evaluating at $\mathcal{S} = \mathbf{1}$, we arrive at

$$\frac{\delta \text{tr}[\hat{P}_{\mathbf{k}}\hat{H}_{\mathbf{k}}^0]}{\langle \delta v_{\mathbf{k}n} |} = \hat{Q}_{\mathbf{k}}\hat{H}_{\mathbf{k}}^0|v_{\mathbf{k}n}\rangle. \quad (\text{C4})$$

Thus the consequence of expressing $\hat{P}_{\mathbf{k}}$ as Eq. (C2) instead of Eq. (43) is to render the gradient orthogonal to the occupied manifold at \mathbf{k} . [When we derived the dynamical equa-

tion (58) using Eq. (47), the gradient of E^0 was not orthogonalized, which is why the dynamics did not follow parallel transport (see Sec. IV C)].

2. Polarization contribution

To find the gradient of the field-coupling term $-v\mathcal{E}\cdot\mathbf{P}$ we need $\delta\bar{\Gamma}_i/\langle\delta v_{\mathbf{k}n}|$. Let us start by recasting Eq. (52) as

$$\bar{\Gamma}_i = \frac{1}{N_i^\perp} \sum_{l=1}^{N_i^\perp} \sum_{j=0}^{N_i^\perp-1} \phi(\mathbf{k}_j^{(i)}, \mathbf{k}_j^{(i)} + \Delta\mathbf{k}_i), \quad (\text{C5})$$

where we have defined the phase

$$\phi(\mathbf{k}, \mathbf{k}') = -\text{Im} \ln \det S(\mathbf{k}, \mathbf{k}'). \quad (\text{C6})$$

Using $\phi(\mathbf{k}', \mathbf{k}) = -\phi(\mathbf{k}, \mathbf{k}')$, this becomes

$$\bar{\Gamma}_i = \frac{1}{N_i^\perp} \sum_{\sigma=\pm 1} \sigma \phi(\mathbf{k}, \mathbf{k}i\sigma) + \dots, \quad (\text{C7})$$

where only the terms depending on $\langle v_{\mathbf{k}n}|$ were written explicitly. Hence

$$\frac{\delta\bar{\Gamma}_i}{\langle\delta v_{\mathbf{k}n}|} = \frac{1}{N_i^\perp} \sum_{\sigma=\pm 1} \sigma \frac{\delta}{\langle\delta v_{\mathbf{k}n}|} \phi(\mathbf{k}, \mathbf{k}i\sigma). \quad (\text{C8})$$

The phase $\phi(\mathbf{k}, \mathbf{k}')$ can be expressed as

$$\begin{aligned} \phi(\mathbf{k}, \mathbf{k}') &= -\text{Im} \text{tr} \ln S(\mathbf{k}, \mathbf{k}') \\ &= \frac{i}{2} \text{tr} \ln S(\mathbf{k}, \mathbf{k}') - \frac{i}{2} \text{tr} \ln S(\mathbf{k}', \mathbf{k}). \end{aligned} \quad (\text{C9})$$

For an arbitrary nonsingular matrix A we have

$$\begin{aligned} \delta \text{tr} \ln A &= \text{tr} \ln(A + \delta A) - \text{tr} \ln(A) \\ &= \text{tr} \ln[(A + \delta A)A^{-1}] \\ &= \text{tr} \ln[1 + (\delta A)A^{-1}] \\ &= \text{tr}[A^{-1}\delta A] + \mathcal{O}(\delta A^2), \end{aligned} \quad (\text{C10})$$

so that

$$\begin{aligned} \frac{\delta \text{tr} \ln S(\mathbf{k}, \mathbf{k}')}{\langle\delta v_{\mathbf{k}n}|} &= \text{tr} \left[S^{-1}(\mathbf{k}, \mathbf{k}') \frac{\delta S(\mathbf{k}, \mathbf{k}')}{\langle\delta v_{\mathbf{k}n}|} \right] \\ &= \sum_{m=1}^M S_{mn}^{-1}(\mathbf{k}, \mathbf{k}') |v_{\mathbf{k}'m}\rangle = |\tilde{v}_{\mathbf{k}'n}\rangle. \end{aligned} \quad (\text{C11})$$

The corresponding derivative of the last term of Eq. (C9) vanishes since $S(\mathbf{k}', \mathbf{k}) = \langle v_{\mathbf{k}'n}|v_{\mathbf{k}n}\rangle$ does not contain $\langle v_{\mathbf{k}n}|$ as a bra. We thus arrive at

$$\frac{\delta \phi(\mathbf{k}, \mathbf{k}')}{\langle\delta v_{\mathbf{k}n}|} = \frac{i}{2} |\tilde{v}_{\mathbf{k}'n}\rangle, \quad (\text{C12})$$

which combined with Eq. (C7) gives

$$\frac{\delta\bar{\Gamma}_i}{\langle\delta v_{\mathbf{k}n}|} = \frac{i}{2N_i^\perp} \sum_{\sigma=\pm 1} \sigma |v_{\mathbf{k}i\sigma,n}\rangle. \quad (\text{C13})$$

This is automatically orthogonal to the occupied manifold at \mathbf{k} . (See Refs. 7 and 10 for alternative derivations.) Collecting terms and using Eq. (57), we obtain Eq. (69) for the gradient of the full energy functional E .

APPENDIX D: DISCRETIZED FORMULA FOR THE CURRENT

Just as the macroscopic polarization \mathbf{P} is evaluated in practice via a finite-difference formula on a mesh of k points, the same can be done for the macroscopic current $\mathbf{J} = d\mathbf{P}/dt$. The invariance of Eq. (27) under the replacement $\partial_{\mathbf{k}} \rightarrow \tilde{\partial}_{\mathbf{k}}$ allows us to then use the discretization rule (60), leading to

$$\mathbf{J} = \frac{e}{4\pi\hbar v} \sum_{n,\mathbf{k}} \sum_{i=1}^3 \sum_{\sigma=\pm 1} \frac{\sigma}{N_i^\perp} \langle v_{\mathbf{k}n} | \hat{H}_{\mathbf{k}}^0 | \tilde{v}_{\mathbf{k}i\sigma,n} \rangle \mathbf{a}_i + \text{c.c.} \quad (\text{D1})$$

We have checked numerically on our one-dimensional tight-binding model that Eq. (D1) yields, for small Δt , the same result as $[P(t+\Delta t) - P(t)]/\Delta t$ computed with the discretized Berry-phase formula.

The same strategy as outlined above can be used to derive a discretized formula for the Berry curvature (25) summed over bands, which is also invariant under $\partial_{\mathbf{k}} \rightarrow \tilde{\partial}_{\mathbf{k}}$. This may be useful in other contexts, such as semiclassical wavepacket dynamics in crystals.⁵⁴

*Present address: NIST Center for Neutron Research and Department of Materials Science and Engineering of the University of Maryland.

¹R.D. King-Smith and D. Vanderbilt, Phys. Rev. B **47**, 1651 (1993).

²M.V. Berry, Proc. R. Soc. London, Ser. A **392**, 45 (1984).

³N. Marzari and D. Vanderbilt, Phys. Rev. B **56**, 12 847 (1997).

⁴R.W. Nunes and D. Vanderbilt, Phys. Rev. Lett. **73**, 712 (1994).

⁵A. Dal Corso and F. Mauri, Phys. Rev. B **50**, 5756 (1994).

⁶A. Dal Corso, F. Mauri, and A. Rubio, Phys. Rev. B **53**, 15 638 (1996).

⁷R.W. Nunes and X. Gonze, Phys. Rev. B **63**, 155107 (2001).

⁸I. Souza, J. Ĩiguez, and D. Vanderbilt, Phys. Rev. Lett. **89**, 117602 (2002).

⁹P. Umari and A. Pasquarello, Phys. Rev. Lett. **89**, 157602 (2002).

¹⁰N. Sai, K.M. Rabe, and D. Vanderbilt, Phys. Rev. B **66**, 104108 (2002).

¹¹S.K. Sundaram and E. Mazur, Nat. Mater. **1**, 217 (2002).

- ¹²See also M. Lazzeri and F. Mauri, Phys. Rev. Lett. **90**, 036401 (2003).
- ¹³J.B. Krieger and G.J. Iafrate, Phys. Rev. B **33**, 5494 (1986); G.J. Iafrate, J.P. Reynolds, J. He, and J.B. Krieger, Int. J. High Speed Electron. Syst. **9**, 223 (1998).
- ¹⁴E.I. Blount, in *Solid State Physics, Advances in Research and Applications*, edited by F. Seitz and D. Turnbull (Academic, New York, 1962), Vol. 13, p. 305, and references cited therein.
- ¹⁵An incorrect interpretation was given in Ref. 7 to the term $ie\mathcal{E} \cdot \partial_{\mathbf{k}}|v_{\mathbf{k}n}\rangle$. It does not come from the “periodic part” of the position operator, but rather from the full position operator, as can be seen from the present derivation.
- ¹⁶After removing the “band” indices Eq. (16) becomes the well-known equation for the k -space dynamics of an electronic wave packet $|\psi\rangle = \int |\phi_{\mathbf{k}}\rangle d\mathbf{k}: \dot{n}_{\mathbf{k}} = (e/\hbar)\mathcal{E} \cdot \partial_{\mathbf{k}}n_{\mathbf{k}}$, where $n_{\mathbf{k}} = \langle v_{\mathbf{k}}|v_{\mathbf{k}}\rangle$. Equation (14) is also valid for such wave packets, even if the derivation given in the text was for WR manifolds.
- ¹⁷Such a coherent “frustrated metal” state can exist in the early moments following a strong femtosecond laser-pulse excitation of a semiconductor, but it will eventually be destroyed by thermal scattering (Ref. 11).
- ¹⁸Y. Aharonov and J. Anandan, Phys. Rev. Lett. **58**, 1593 (1987).
- ¹⁹The resemblance of Eqs. (24) and (25) to the so-called anomalous current (Ref. 54) in semiclassical wave-packet dynamics is misleading, since the Berry curvature entering the anomalous current pertains to the band states $|u_{\mathbf{k}n}\rangle$, not to $|v_{\mathbf{k}n}\rangle$. In fact, it can be shown that the anomalous current is contained in the other term, Eq. (27), once it is properly modified for wave packets.
- ²⁰W. Kohn, Phys. Rev. **133**, A171 (1964); W. Kohn, in *Many-Body Physics*, edited by C. DeWitt and R. Balian (Gordon and Breach, New York, 1968), p. 351.
- ²¹I. Souza, T. Wilkens, and R.M. Martin, Phys. Rev. B **62**, 1666 (2000).
- ²²R. Resta and S. Sorella, Phys. Rev. Lett. **82**, 370 (1999).
- ²³H. Goldstein, *Classical Mechanics*, 2nd ed. (Addison-Wesley, Reading, MA, 1980).
- ²⁴E. Fradkin, *Field Theories of Condensed Matter Systems* (Addison-Wesley, Reading, MA, 1991).
- ²⁵Note that for a purely electronic wave packet $\psi(\mathbf{r}) = \int e^{i\mathbf{k}\cdot\mathbf{r}}v_{\mathbf{k}}(\mathbf{r})d\mathbf{k}$ the property $\partial_{\mathbf{k}}\langle v_{\mathbf{k}}|v_{\mathbf{k}}\rangle = 0$ does not hold and hence $(A_{\mathbf{k}}^{\alpha})^* \neq A_{\mathbf{k}}^{\alpha}$. As a consequence, unlike Eq. (14), which correctly describes the dynamics of wave packets (Ref. 16) Eq. (41) is only valid for WR manifolds. Of course, when wave packets of *electron-hole pairs* are created by vertical electronic transitions in k space, the electronic manifold remains Wannier representable, and can be described within the present formalism (see, e.g., Sec. VI B).
- ²⁶S.E. Koonin and D.C. Meredith, *Computational Physics* (Addison-Wesley, Reading, MA, 1990).
- ²⁷O. Sugino and Y. Miyamoto, Phys. Rev. B **59**, 2579 (1999).
- ²⁸N. Watanabe and M. Tsukada, Phys. Rev. E **65**, 036705 (2002).
- ²⁹G. Nenciu, Rev. Mod. Phys. **63**, 91 (1991).
- ³⁰J. Íñiguez, I. Souza, and D. Vanderbilt (unpublished).
- ³¹G. Wannier, Phys. Rev. **100**, 1227 (1955); **101**, 1835 (1956).
- ³²E.N. Adams, Phys. Rev. **107**, 698 (1957).
- ³³J.M. Soler *et al.*, J. Phys.: Condens. Matter **14**, 2745 (2002).
- ³⁴J. Bennetto and D. Vanderbilt, Phys. Rev. B **53**, 15 417 (1996).
- ³⁵D.H. Dunlap and V.M. Kenkre, Phys. Rev. B **34**, 3625 (1986).
- ³⁶B.A. Foreman, Phys. Rev. B **66**, 165212 (2002), and references cited therein.
- ³⁷D.J. Thouless, Phys. Rev. B **27**, 6083 (1983).
- ³⁸It may seem surprising that even though we use a discrete mesh of k points—which effectively turns the system into a finite torus—our calculations display exact quantization of adiabatic particle transport. According to Thouless (Ref. 37) this should only occur in the thermodynamic (continuum- k) limit. This has to do with our using the discretized Berry-phase formula (52), which is not fully consistent with the velocity operator (30) on the finite torus (we recall that the derivation in Sec. III A was done in the continuum- k limit). From this viewpoint it seems preferable to regard the discretization procedure as a numerical approximation to the continuum- k limit, rather than as an exact calculation on the finite torus.
- ³⁹In the limit where the number N of k points is large, ξ is finite for the ground state of insulators and diverges for that of metals (Ref. 21). For finite N it cannot really diverge. In particular, when $\xi = (\Omega_1/M)^{1/2}$ is evaluated using Eq. (34) of Marzari and Vanderbilt (Ref. 3) it cannot exceed, in one dimension, $aN/2\pi$, well above the values that we observe in all our simulations.
- ⁴⁰J.J. O’Dwyer, *The Theory of Electrical Conduction and Breakdown in Solid Dielectrics* (Clarendon, Oxford, 1973), p. 13.
- ⁴¹E.O. Kane, J. Phys. Chem. Solids **12**, 181 (1959).
- ⁴²P.Y. Yu and M. Cardona, *Fundamentals of Semiconductors* (Springer, Berlin, 1996).
- ⁴³S. Schmitt-Rink, D.S. Chemla, and D.A.B. Miller, Adv. Phys. **38**, 89 (1989).
- ⁴⁴M. Ando *et al.*, Superlattices Microstruct. **22**, 459 (1998).
- ⁴⁵A. Tsolakidis, D. Sánchez-Portal, and R.M. Martin, Phys. Rev. B **66**, 235416 (2002).
- ⁴⁶K. Yabana and G.F. Bertsch, Int. J. Quantum Chem. **75**, 55 (1999).
- ⁴⁷G.F. Bertsch, J.-I. Iwata, A. Rubio, and K. Yabana, Phys. Rev. B **62**, 7998 (2000).
- ⁴⁸W. Jones and N.H. March, *Theoretical Solid State Physics* (Wiley, New York, 1973), Vol. 1.
- ⁴⁹Since $\delta(\mathbf{k}-\mathbf{k}')$ has units of real-space volume, the right-hand side of Eq. (A1) is dimensionless. In the discrete- k case the integral on the left-hand side is over the supercell volume $V = Nv$, and $\Omega_B\delta(\mathbf{k}-\mathbf{k}')$ is replaced by $N\delta_{\mathbf{k}\mathbf{k}'}$.
- ⁵⁰J.E. Sipe and A.I. Shkrebtii, Phys. Rev. B **61**, 5337 (2000).
- ⁵¹W.R.L. Lambrecht and S.N. Rashkeev, Phys. Status Solidi B **217**, 599 (2000).
- ⁵²J. Callaway, *Quantum Theory of the Solid State*, 2nd ed. (Academic Press, New York, 1991).
- ⁵³C. Aversa and J.E. Sipe, Phys. Rev. B **52**, 14 636 (1995).
- ⁵⁴M.C. Chang and Q. Niu, Phys. Rev. B **53**, 7010 (1996).